



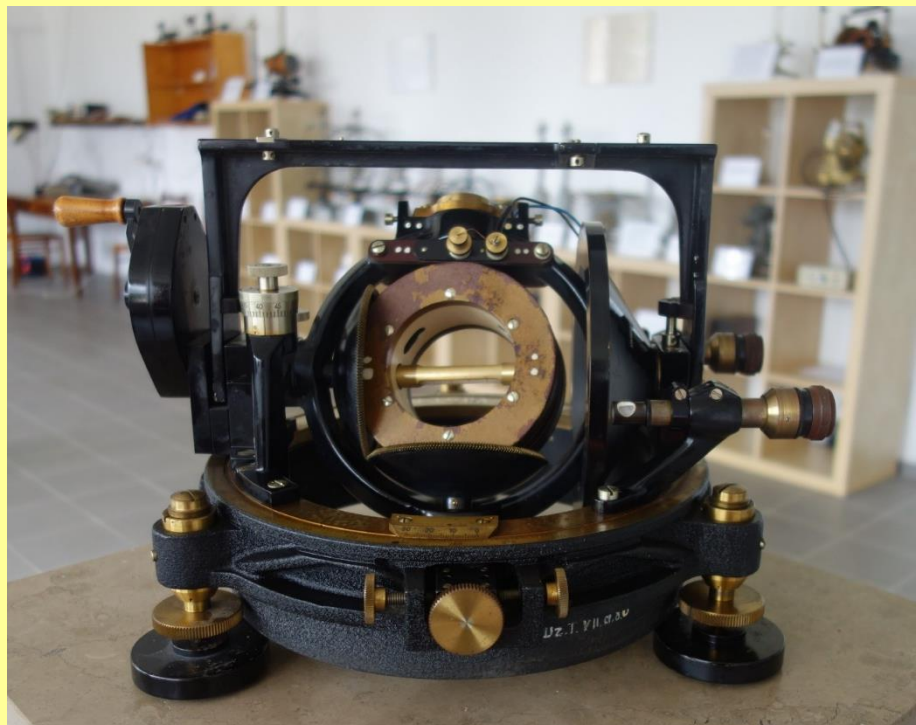
Institute of Geophysics
Polish Academy of Sciences

**PUBLICATIONS
OF THE INSTITUTE OF GEOPHYSICS
POLISH ACADEMY OF SCIENCES**

Geophysical Data Bases, Processing and Instrumentation

448 (C-117)

**Results of Geomagnetic Observations:
Belsk, Hel, Hornsund, 2022**



Warsaw 2023 (Issue 5)

**INSTITUTE OF GEOPHYSICS
POLISH ACADEMY OF SCIENCES**

**PUBLICATIONS
OF THE INSTITUTE OF GEOPHYSICS
POLISH ACADEMY OF SCIENCES**

Geophysical Data Bases, Processing and Instrumentation

448 (C-117)

**Results of Geomagnetic Observations:
Belsk, Hel, Hornsund, 2022**

Warsaw 2023

Editor-in-Chief

Marek KUBICKI

Advisory Editorial Board

Janusz BORKOWSKI (Institute of Geophysics, PAS)

Tomasz ERNST (Institute of Geophysics, PAS)

Maria JELEN SKA (Institute of Geophysics, PAS)

Andrzej KIJKO (University of Pretoria, Pretoria, South Africa)

Natalia KLEIMENOVA (Institute of Physics of the Earth, Russian Academy of Sciences, Moscow, Russia)

Zbigniew KŁOS (Space Research Center, Polish Academy of Sciences, Warsaw, Poland)

Jan KOZAK (Geophysical Institute, Prague, Czech Republic)

Antonio MELONI (Istituto Nazionale di Geofisica, Rome, Italy)

Hiroyuki NAGAHAMA (Tohoku University, Sendai, Japan)

Kaja PIETSCH (AGH University of Science and Technology, Cracow, Poland)

Paweł M. ROWIŃSKI (Institute of Geophysics, PAS)

Steve WALLIS (Heriot Watt University, Edinburgh, United Kingdom)

Waclaw M. ZUBEREK (University of Silesia, Sosnowiec, Poland)

Associate Editors

Łukasz RUDZIŃSKI (Institute of Geophysics, PAS) – **Solid Earth Sciences**

Jan WISZNIOWSKI (Institute of Geophysics, PAS) – **Seismology**

Jan REDA (Institute of Geophysics, PAS) – **Geomagnetism**

Krzysztof MARKOWICZ (Institute of Geophysics, Warsaw University) – **Atmospheric Sciences**

Mark GOŁKOWSKI (University of Colorado Denver) – **Ionosphere and Magnetosphere**

Andrzej KUŁAK (AGH University of Science and Technology) – **Atmospheric Electricity**

Marzena OSUCH (Institute of Geophysics, PAS) – **Hydrology**

Adam NAWROT (Institute of Geophysics, PAS) – **Polar Sciences**

Managing Editor

Anna DZIEMBOWSKA

Technical Editor

Marzena CZARNECKA

Published by the Institute of Geophysics, Polish Academy of Sciences

ISBN 978-83-66254-20-6 eISSN-2299-8020

DOI: 10.25171/InstGeoph_PAS_Publs-2023-025

Photo on the front cover by Jan Reda

Editorial Office
Instytut Geofizyki Polskiej Akademii Nauk
ul. Księcia Janusza 64, 01-452 Warszawa

Results of Geomagnetic Observations Belsk, Hel, Hornsund, 2022

Jan REDA[✉], Mariusz NESKA, Stanisław WÓJCIK, and Paweł CZUBAK

Institute of Geophysics, Polish Academy of Sciences, Warsaw, Poland

[✉] jreda@igf.edu.pl

1. INTRODUCTION

This publication contains basic information on geomagnetic observations carried out in 2022 in three Polish geophysical observatories: Belsk, Hel, and Hornsund. IAGA codes are respectively: BEL, HLP, and HRN. All these observatories belong to the Institute of Geophysics, Polish Academy of Sciences. Observatories Belsk and Hel are located on the territory of Poland, while Hornsund is in Spitsbergen archipelago, under Norwegian administration.

In 2022, like in the previous years, the Belsk, Hel, and Hornsund observatories have kept a close collaboration with the world network of geomagnetic observatories INTERMAGNET. The Belsk Observatory joined INTERMAGNET in 1992, Hel in 1999, and Hornsund in 2002. Data of geomagnetic field components XYZF have been sent to the INTERMAGNET centre in real time so they are publicly available on the Internet. At the beginning of 2023 have been prepared the final data (status Definitive) for the whole 2022 year observations. Definitive Data are published on INTERMAGNET website too.

Both the Polish Polar Station Hornsund and Hel Observatory are working for the IMAGE program. The primary objective of IMAGE is to study auroral electrojets and moving two-dimensional current systems.

Belsk and Hel observatories are providing their data, both real-time and final, to EMMA network (European quasi-Meridional Magnetometer Array). These data are exploited for investigation of the plasmasphere.

2. WHAT IS OBSERVED

Magnetic observatories continuously measure the strength and direction of the Earth's magnetic field over many years (Macmillan 2007).

The Earth's magnetic field can be divided into two components:

- a slowly changing large part called the main field,
- the external field, which usually has 1–10% of the main field and is characterized by relatively rapid changes.

For the above reason, the instrumentation of geomagnetic observatories is twofold. Extensive effort is paid to determine with high accuracy the absolute measurements of the Earth's field, which is essential for observing the Earth's main field. It is mainly due to absolute measurements we can reliably observe secular changes of the Earth's magnetic field. On the other hand, changes of geomagnetic field are recorded with relative instruments, the so-called variometers (Geese 2011).

For all three Polish observatories, we record changes in the XYZF components of the geomagnetic field (Fig. 1) and perform absolute measurements of Declination, Inclination, and total field F .

The described duality is also reflected in the observatory buildings. Absolute measurements and registration of magnetic field changes are carried out in separate non-magnetic buildings: the absolute house (e.g. Figs. 3 and 5) and the variometer house (e.g. Fig. 5).

One of the most important products of a multi-stage observational effort is time series data of the Definitive type. It is kind of combination of data from variometers and absolute measurements. This involves correcting variometer data with adopted baselines obtained from absolute measurements. This publication is prepared based on Definitive-type data.

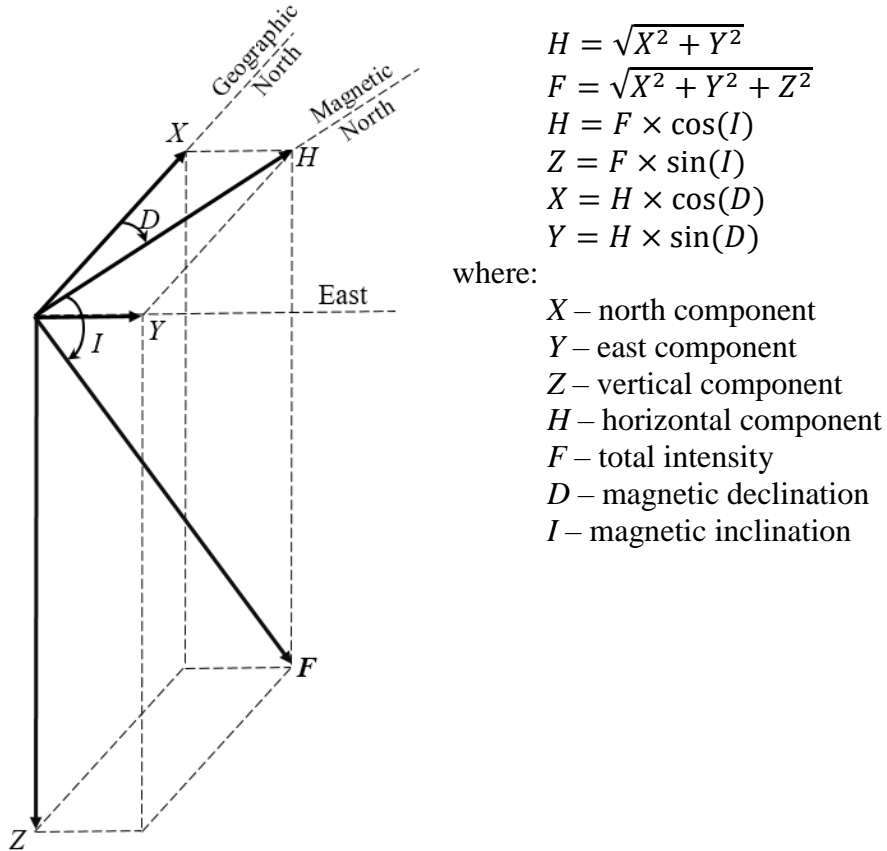


Fig. 1. Components of the Earth's magnetic field and the relations between them.

3. DESCRIPTION OF OBSERVATORIES

The location of observatories is shown in Fig. 2 and Table 1. The geomagnetic coordinates in Table 1 were calculated on the basis of model IGRF-13 from epoch 2022.5 (http://www.geomag.bgs.ac.uk/data_service/models_compass/coord_calc.html).

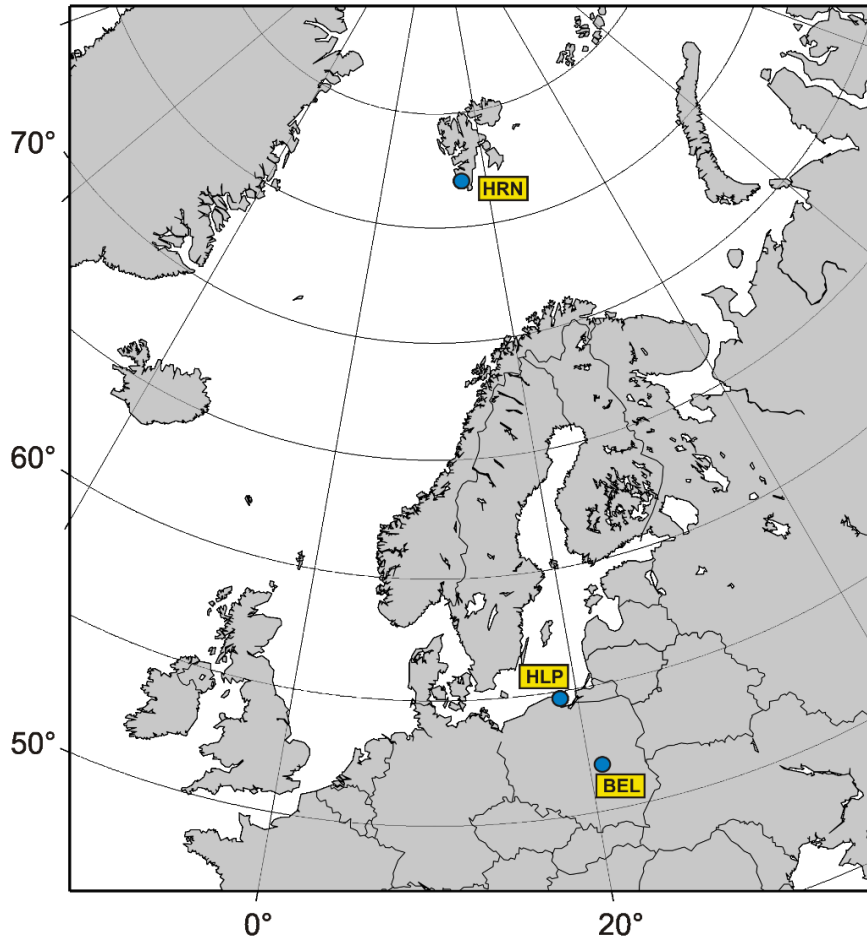


Fig. 2. Location of the Belsk, Hel, and Hornsund observatories.

Table 1
Coordinates of the Polish observatories

Observatory	Geographic coordinates		Geomagnetic coordinates		Elevation [m]
	Latitude	Longitude	Latitude	Longitude	
Belsk (BEL)	51° 50.2' N	20° 47.3' E	50.36° N	104.78° E	180
Hel (HLP)	54° 36.2' N	18° 48.6' E	53.34° N	104.09° E	1
Hornsund (HRN)	77° 0.0' N	15° 33.0' E	74.34° N	123.58° E	15

The methodology of geomagnetic observations in all three observatories was very similar, based on the *Guide for Magnetic Measurements and Observatory Practice* (Jankowski and Sucksdorff 1996). The instruments were similar too. Absolute measurements were made with the use of DI-flux magnetometers and proton magnetometers. In turn, the magnetic field variations were measured with the use of GEOMAG and LEMI flux-gate magnetometers.

Continuous recording has been made by means of digital loggers type NDL. Due to the hardware and organizational solutions used, gaps in one-minute XYZ components from Belsk and Hel are practically absent.

It is worth mentioning that in 2022 the Hornsund and Suwałki stations have been continuing the permanent observation of the Schumann resonance phenomenon. Two horizontal magnetic components have been recorded at a frequency of 100 Hz. This recording was initiated in 2004 (Neska and Satori 2006).

3.1 Central Geophysical Observatory at Belsk, Central Poland

The Observatory at Belsk began continuous observations of the Earth magnetic field in 1965 (Jankowski and Maraniuk 2007). It continued the activity of the first Polish magnetic Observatory at Świder near Warsaw, working incessantly through the years 1920–1975. The magnetic observations were transferred from Świder to Belsk because of a strong increase of artificial noise from the Warsaw agglomeration, in particular due to the electric railroad passing nearby the Świder Observatory.



Fig. 3. Belsk Observatory – Absolute House.

The Belsk Observatory is located at a distance of about 50 km south of Warsaw and about 2 km northwest of the village Belsk Duży. The premises of the Observatory, about 10 ha in area, is at the edge of the forest reserve Modrzewina, far away of people's settlements and automobile traffic. The Observatory is surrounded by typically agricultural regions (with fertile soil, mostly apple orchards), so the direct neighborhood is deprived of sources of major artificial geomagnetic field disturbances. It is only the electric railroad (DC powered) situated some 14 km away of the Observatory to the north that produces some small artificial magnetic disturbances, whose average level usually does not exceed 1 nT.

More information about the region in which the Observatory is located can be found on the internet pages of Grójec district (https://en.wikipedia.org/wiki/Gr%C3%B3jec_County) to which the village Belsk Duży belongs. Relevant information about Belsk Observatory can be found at page: <http://www.igf.edu.pl/>.

3.2 Geophysical Observatory at Hel, Northern Poland

The Observatory at Hel (Fig. 4) began continuous observations of the earth magnetic field in 1932 (Jankowski and Marianuk 2007). The observations were stopped in 1939, after the outbreak of World War II. During the war, the Observatory as well as its equipment and data were completely destroyed. After reconstruction, continuous observations at Hel were resumed in 1953.

The Hel Observatory is located in a small resort town at the end of Hel Peninsula by the Bay of Gdańsk. It is the area of Seaside Landscape Park (Nadmorski Park Krajobrazowy), weakly industrialized and urbanized. The region, surrounded by water from three sides, lacks any major artificial noise and is a good place for continuous magnetic observations.

The observatory premises, about 4.5 ha in area, is surrounded by mixed forest (mainly pine and birch trees). Pavilions with measurement and recording instruments are located at small clearings.

More information about the town of Hel where the Observatory is located can be found at the address: http://en.wikipedia.org/wiki/Hel,_Poland.



Fig. 4. Hel Observatory – Variometer House.

3.3 Polish Polar Station Hornsund, Spitsbergen

The Polish Polar Station Hornsund (PSP Hornsund, Fig. 5) is situated on the White Bear Bay (Isbjørnhamna) in Hornsund Fiord, Spitsbergen Island, Svalbard archipelago. More information on the Svalbard Archipelago can be found at the address: <http://en.wikipedia.org/wiki/Svalbard>. The Hornsund Station is the northernmost Polish scientific facility carrying out year-round activity. The Hornsund region is situated in a zone of strong magnetic field activity, much stronger than on the magnetic pole. Therefore, it is a very interesting place for magnetic observations.

Polish geomagnetic observations in the Arctic were initiated during the II Polar Year; a magnetic station was then established by S. Siedlecki and C. Centkiewicz on the Bear Island. In the years 1932–1933, they had carried out continuous recording of magnetic field and performed absolute measurements. Unfortunately, all data were destroyed during the war. In the years 1957–1958, in the framework of the International Geophysical Year, measurements of magnetic declination and inclination were made by J. Kowalcuk and K. Karaczun in five sites in the Hornsund Fiord region.



Fig. 5. The Variometer House (left) and the Absolute House (right) in PSP Hornsund, Spitsbergen.

Since the beginning of October 1978, continuous magnetic field recording has been put into operation, and systematic absolute measurements have been implemented (Jankowski and Marianiuk 2007). Since then, PSP Hornsund has begun to fulfill all the requirements for geomagnetic observatory.

Since 1993, PSP Hornsund has been participating in the IMAGE (International Monitor for Auroral Geomagnetic Effects) project. In the framework of this project, Hornsund data are being sent to Finnish Meteorological Institute once a month on the average and available on <http://www.geo.fmi.fi/image/request.html>. Since 2002, PSP Hornsund is included into the global near-real-time magnetic observatory network INTERMAGNET, sending the results, via Internet, to the GIN (Geomagnetic Information Nodes) center in Edinburgh.

4. INSTRUMENTATION

4.1 Absolute measurements

In all the three Polish observatories, the absolute measurements used for determination of bases of the recordings are performed by means of *DI*-flux and proton magnetometers. *DI*-flux magnetometers measure the absolute values of the angles of declination *D* and inclination *I*, while the proton magnetometers measure the absolute values of the total magnetic field vector *F*. From the measured values of *F*, *D*, and *I*, we can calculate all the remaining magnetic field components, *H*, *X*, *Y*, and *Z*.

The results of absolute measurements are determined by means of a special computer package ABS written in Java (author: M. Neska), which calculates the base values on the basis of data from the measurement protocol.

The instruments for absolute measurements are listed in Table 2, and the basic parameters of the instruments in Table 3.

Table 2
Instruments for absolute measurements

	Belsk	Hel	Hornsund
DI-fluxgate (fluxgate, theodolite)	GEOMAG-03 THEO-010B sn: 07-2019	FLUX-9408 THEO-10B sn: 160334	GEOMAG-03 THEO-010B sn: 03-2012
Proton magnetometer	GSM-90 sn: 9038262/96334	PMP-8 sn: 21/2006	PMP-5 sn: 115
Frequency of measurements	3, 4 per week	3 per week	2 per week

Table 3
Basic parameters of the instruments for absolute measurements

Fluxgate declinometer/inclinometer GEOMAG 03 / THEO-010B	
Producer	GEOMAGNET, Ukraine
Mean square error of a horizontal direction	$\sigma_D \approx \pm 5''$
Mean square error of a zenith direction	$\sigma_I \approx \pm 5''$
Fluxgate declinometer/inclinometer ELSEC 810 / THEO-010B	
Producer	ELSEC Oxford, UK
Mean square error of a horizontal direction	$\sigma_D \approx \pm 5''$
Mean square error of a zenith direction	$\sigma_I \approx \pm 5''$
Fluxgate declinometer/inclinometer FLUX-9408 / THEO-010B	
Producer (FLUX-9408)	Institute of Geophysics Pol. Acad. Sc.
Mean square error of a horizontal direction	$\sigma_D \approx \pm 5''$
Mean square error of a zenith direction	$\sigma_I \approx \pm 5''$
Proton magnetometer model PMP-5	
Producer	Institute of Geophysics Pol. Acad. Sc.
Resolution	0.1 nT
Absolute accuracy	0.2 nT
Proton magnetometer model PMP-8	
Producer	Institute of Geophysics Pol. Acad. Sc.
Resolution	nT
Absolute accuracy	0.2 nT
Overhauser magnetometer model GSM-90	
Producer	GEM Systems, Canada
Resolution	0.01 nT
Absolute accuracy	0.2 nT

Results of base determinations and the smoothed values adopted for further computations are depicted in Figs. 6, 9, and 12 in the chapters describing individual observatories.

Table 4
Mean errors of measurements of B_X , B_Y , B_Z , and B_F in 2022

Observatory	Component	Number of measurements n	Mean error m_B [nT]
Belsk	B_X	157	0.50
	B_Y	157	0.48
	B_Z	162	0.23
Hel	B_X	151	0.35
	B_Y	154	0.36
	B_Z	155	0.26
Hornsund	B_X	101	1.28
	B_Y	97	1.57
	B_Z	156	0.70

The mean random errors of a single base measurement, m_B , and the number of measurements n taken in 2022 are listed in Table 4.

Thermal coefficients of magnetic sensors are not taken into account in calculations, with a view to the following facts:

- tests made every few years indicated that the coefficients are very small, less than 0.2 nT/°C,
- the magnetic sensors are located in thermostat-controlled wooden boxes where the daily temperature variations are of the order of 0.3°C.

4.2 Recording of geomagnetic field variations

As we already mentioned, the continuous digital recordings of geomagnetic field variations in all the Polish observatories are performed by means of magnetometers equipped with flux-gate sensors (GEOMAG, LEMI) and digital loggers NDL. In spare sets, we use LEMI magnetometers. Both the main and spare sets record the components in the rectangular coordinate system X , Y , Z . At Belsk and Hel, continuous recording of the total magnetic field modulus F is performed as well. The basic parameters of the recording systems are listed in Tables 5a, 5b, 5c.

GEOMAG and LEMI magnetometers

The magnetometers of GEOMAG and LEMI type were designed at the GEOMAGNET company and the Lviv Centre of the Institute of Space Research, respectively, in Ukraine. They employ flux-gate sensors. They are characterized by good orthogonality of sensors and relatively small self noise.

Proton magnetometers PMP-5 and PMP-8

The magnetometers of type PMP-5 and PMP-8 were designed at the Institute of Geophysics PAS. These are classical proton magnetometers, in which the precession signal is forced in a cycle of proton polarization by means of direct current. The resolution of magnetometers PMP-5 is 0.1 nT, that of PMP-8 being 0.01 nT. The stability of both magnetometers is better than 0.3 nT/year. The calibration of proton magnetometers is performed according to the method described by Reda and Neska (2007).

Table 5a
Basic instruments for the magnetic field variations recording in Belsk Observatory

Set / Period	Parameter name	Value
Set 1 Vector magnetometer	Name of magnetometer	GEOMAG-02
	Kind of sensor	Fluxgate
	Serial No.	No. 37
	Sensor's orientation	XYZ
	Range	+/- 3200 nT
	Magnetometer's producer	GEOMAGNET
	Digital recorder	NDL
	Producer	TUS Electronics
Set 2 Vector magnetometer	Sampling interval	1 s
	Name of magnetometer	GEOMAG-02
	Kind of sensor	Fluxgate
	Serial No.	No. 39
	Sensor's orientation	XYZ
	Range	+/- 3200 nT
	Magnetometer's producer	GEOMAGNET
	Digital recorder	NDL
Set 1 Scalar magnetometer	Producer	TUS Electronics
	Sampling interval	1 s
	Name of magnetometer	GSM-90
	Kind of sensor	Overhauser proton magnetometer
	Serial No.	No. 9038261
Set 1 Scalar magnetometer	Magnetometer's producer	GEM Systems
	Sampling interval	1 s

GSM-90 scalar magnetometer

The Canadian GSM-90 is a scalar Overhauser effect magnetometer characterized by high absolute accuracy (0.2 nT) and a low long-term drift (0.05 nT/year). Therefore it is ideally suited for continuous recording of total field F in magnetic observatories.

NDL digital data loggers

The NDL data logger is designed for recording of analog signals, mainly coming from geophysical phenomena detectors. The instrument is equipped with six independent measuring channels; the analog-to-digital conversion is realized using 24 bit sigma-delta converters. The GPS receiver ensures high time accuracy of recorded signals. The NDL is equipped with ftp server; this allows easy access to NDL via Internet.

Table 5b
Basic instruments for the magnetic field variations recording in Hel Observatory

Set / Period	Parameter name	Value
Set 1 Vector magnetometer	Name of magnetometer	GEOMAG-02
	Kind of sensor	Fluxgate
	Serial No.	No. 25
	Sensor's orientation	XYZ
	Range	+/- 3200 nT
	Magnetometer's producer	GEOMAGNET
	Digital recorder	NDL
	Producer	TUS Electronics
	Sampling interval	1 s
Set 2 Vector magnetometer	Name of magnetometer	LEMI-03/95
	Kind of sensor	Fluxgate
	Serial No.	No. 03
	Sensor's orientation	XYZ
	Range	+/- 1000 nT
	Magnetometer's producer	Lviv Centre of the Institute of Space Research
	Digital recorder	LB-480
	Producer	LAB-EL
	Sampling interval	1 s
Set 1 Scalar magnetometer	Name of magnetometer	GSM-90
	Kind of sensor	Overhauser proton magnetometer
	Serial No.	No. 9038264
	Magnetometer's producer	GEM Systems
	Sampling interval	1 s

LB-480 digital data loggers

The LB-480 is equipped with 24-bits sigma-delta A/D converter, GPS receiver, Ethernet and USB interfaces, and GSM modem. The logger allows simultaneously record up to 6 analog signals, and can be used in geophysics.

4.3 Calibration of magnetic sensors

The verification of scale values of recording systems in all three observatories was made by the classical electromagnetic method: electric currents were passed through calibration coils woven over variometers. The currents induce the magnetic field of precisely known intensity. The measurements are made at least few times a year.

Table 5c
Basic instruments for the magnetic field variations recording in Hornsund Observatory

Set / Period	Parameter name	Value
Set 1 Vector magnetometer	Name of magnetometer	LEMI-03
	Kind of sensor	Fluxgate
	Serial No.	No. 12
	Sensor's orientation	XYZ
	Range	+/- 10000 nT
	Magnetometer's producer	Lviv Centre of the Institute of Space Research
	Digital recorder	NDL
	Producer	TUS Electronics
	Sampling interval	1 s
Set 2 Vector magnetometer	Name of magnetometer	GEOMAG-02
	Kind of sensor	Fluxgate
	Serial No.	No. 40
	Sensor's orientation	XYZ
	Range	+/- 3200 nT
	Magnetometer's producer	GEOMAGNET
	Digital recorder	NDL
	Producer	TUS Electronics
	Sampling interval	1 s
Set 1 Scalar magnetometer	Name of magnetometer	GSM-90
	Kind of sensor	Overhauser proton magnetometer
	Serial No.	No. 9038263
	Magnetometer's producer	GEM Systems
	Sampling interval	1 s

The scale values of magnetometers GEOMAG, and LEMI and mutual orthogonality of sensors in magnetometers is checked every few years in large calibration coils installed at the Belsk Observatory.

4.4 Data processing

In processing the results of digital recordings we used the software packet developed for the needs of an observatory operating in the INTERMAGNET network. This software makes it possible to perform, among other things, the following operations:

- conversion of magnetic data into the INTERMAGNET binary format IAF and creation in this format of monthly files containing one-minute means of X , Y , Z , and ΔF (author: M. Neska),

- automatic transmission of data, via the Internet, to the Institute of Geophysics PAS in Warsaw and data centers in Edinburgh (author: M. Neska),
- archiving of data and plotting of magnetograms (authors: J. Reda, M. Neska, S. Wójcik),
- calculation of results of absolute measurements (author: M. Neska),
- automatic calculation of geomagnetic indices K (Nowożyński *et al.* 1991). The indices are calculated with the use of ASm (Adaptive Smoothed) method, developed at the Institute of Geophysics PAS, and recommended by IAGA in 1991. The currently used program calculates the indices from one-minute means in the IAF Format (INTERMAGNET Archive Format) or in the IMFV1.23 format. The program for calculation of indices may be taken from the INTERMAGNET page: <http://www.intermagnet.org/publication-software/software-eng.php>,
- test printouts to check various parameters of recording adopted for calculation and a possibility of looking over current and past data curves or tables.

The diagrams illustrating the annual variations of X , Y , and Z (Figs. 7, 10, and 13), bases of recording sets as well as plots of K indices for 2022 (Figs. 8, 11, and 14) were prepared with the use of program imcdview.jar.

As in previous years, we include the E indices calculated for Belsk observatory in the present yearbook (Tables 12–15). The E indices, unlike the K indices, are calculated on the basis of energy analysis. They have been described in detail by Reda and Jankowski (2004).

Annual mean values for Belsk, Hel, and Hornsund are listed in Tables 6, 16, and 22, respectively. Monthly mean values of 2022 for Belsk, Hel, and Hornsund are listed in Tables 7, 17, and 23, respectively.

Three-hour-range K indices for Belsk are listed in Tables 8–11, for Hel in Tables 18–21, and for Hornsund in Tables 24–27.

4.5 Data availability

The newest data from Belsk, Hel, and Hornsund observatories can be viewed in graphic form through the WEB application: <http://rtbel.igf.edu.pl> described by Nowożyński and Reda (2007).

On this page, the Belsk and Hel data appear with one-hour delay, while the delay for Hornsund is few hours. The page makes it possible to view the archival data from any observatory belonging to the INTERMAGNET network (in the form of curves on the screen). It offers also a possibility of calculating the K indices according to the ASm method (Nowożyński *et al.* 1991) and E indices (Reda and Jankowski 2004).

The current data (of status REPORTED) from all three observatories can be found in INTERMAGNET at the Internet address: <http://www.intermagnet.org>.

Data from Belsk, Hel, and Hornsund are also available from the WDCs. Addresses of some WDC pages with magnetic data are the following:

- WDC for Geomagnetism, Edinburgh <http://www.wdc.bgs.ac.uk/catalog/master.html>,
- WDC for Geomagnetism, Kyoto <https://wdc.kugi.kyoto-u.ac.jp/>.

All the three observatories have in their archives the original data, whose sampling periods are listed in Tables 5a, 5b, 5c. For those interested, these data can be made available on request.

5. CONTACT PERSONS, POSTAL ADDRESSES, CONTACT DETAILS

5.1 Belsk Observatory

Jan Reda, Mariusz Neska
Central Geophysical Observatory
05-622 Belsk
Poland
Tel.: +48 486610830
E-mails: jreda@igf.edu.pl (J. Reda), nemar@igf.edu.pl (M. Neska)
<http://www.igf.edu.pl/>

5.2 Hel Observatory

Stanisław Wójcik
Geophysical Observatory
ul. Sosnowa 1
84-150 Hel
Poland
Tel./Fax +48 58 6750480
E-mail: hel@igf.edu.pl
<http://www.igf.edu.pl/>

5.3 Hornsund Observatory

Mariusz Neska, Paweł Czubak
Central Geophysical Observatory
05-622 Belsk
Poland
Tel.: +48 486610833
E-mails: nemar@igf.edu.pl (M. Neska), pczubak@igf.edu.pl (P. Czubak)
<http://hornsund.igf.edu.pl/>
<http://www.igf.edu.pl/>

6. PERSONNEL TAKING PART IN THE WORK OF BELSK, HEL, AND HORNSUND OBSERVATORIES IN 2022

Jan Reda (project leader of geomagnetic observations in Belsk, Hel, Hornsund)
Paweł Czubak
Krzysztof Kucharski
Tomasz Ślęczkowski (Hornsund, observer in the 1-st half-of 2022)
Mariusz Neska
Robert Szymko (Hornsund, observer in the 2-nd half-of 2022)
Anna Wójcik
Stanisław Wójcik

7. TABLES AND PLOTS FOR BELSK OBSERVATORY

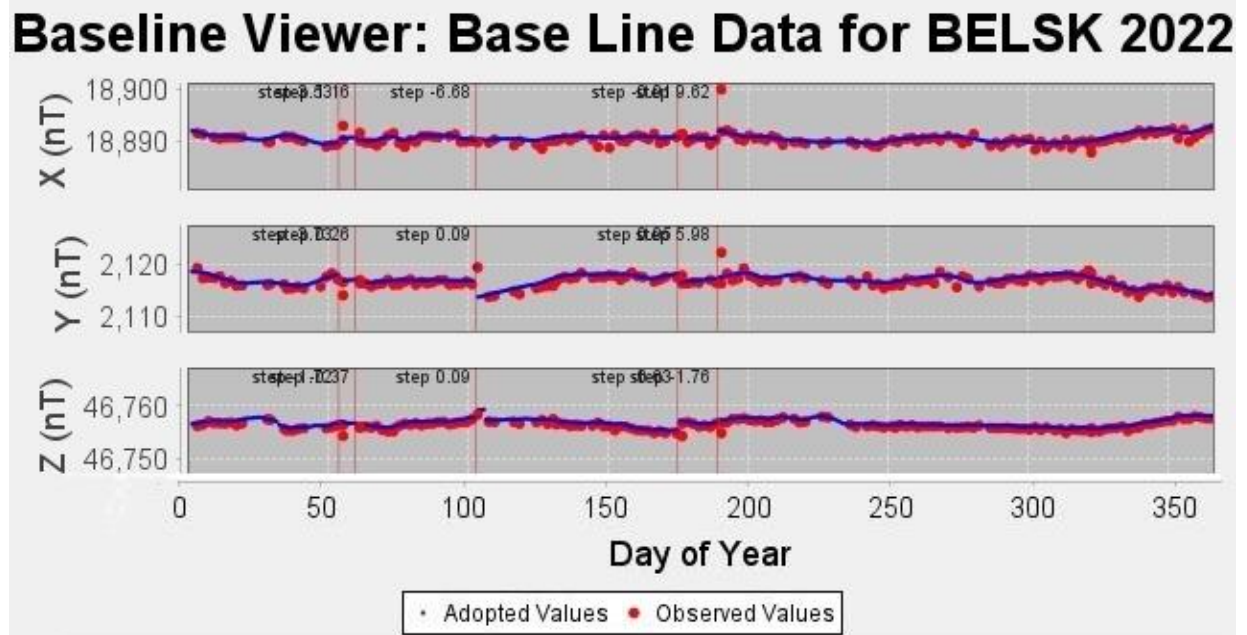


Fig. 6. Base values of set 1, Belsk 2022.

Table 6
Annual mean values of magnetic components in Belsk Observatory

No.	Year	D [°']	H [nT]	Z [nT]	X [nT]	Y [nT]	I [°']	F [nT]
1	1966	2 04.2	18901	45023	18889	683	67 13.6'	48830
2	1967	2 05.6	18906	45048	18894	691	67 14.0	48854
3	1968	2 06.2	18917	45071	18906	695	67 13.8	48880
4	1969	2 06.3	18935	45094	18923	696	6713.3	48908
5	1970	2 06.6	18953	45123	18940	698	67 13.0	48942
6	1971	2 06.6	18976	45146	18963	699	67 12.2	48972
7	1972	2 08.0	18992	45176	18978	707	67 11.9	49006
8	1973	2 10.2	19005	45211	18991	719	67 12.0	49043
9	1974	2 13.3	19016	45246	19002	737	67 12.2	49079
10	1975	2 16.4	19035	45274	19020	755	67 11.7	49112
11	1976	2 18.5	19050	45307	19034	767	67 11.7	49149
12	1977	2 22.0	19062	45337	19046	787	67 11.7	49181
13	1978	2 27.4	19059	45376	19041	817	67 13.0	49216
14	1979	2 32.3	19061	45401	19043	844	67 13.5	49240
15	1980	2 37.2	19063	45418	19043	871	67 13.9	49257
16	1981	2 42.9	19047	45449	19026	902	67 15.7	49279
17	1982	2 48.3	19035	45479	19012	931	67 17.3	49302
18	1983	2 52.4	19033	45499	19009	954	67 18.0	49319

to be continued

Table 6 (continuation)
Annual mean values of magnetic components in Belsk Observatory

No.	Year	D [°']	H [nT]	Z [nT]	X [nT]	Y [nT]	I [°']	F [nT]
19	1984	2 56.9	19023	45520	18998	978	67 19.2	49335
20	1985	3 00.8	19015	45542	18989	999	67 20.3	49352
21	1986	3 05.1	19003	45570	18976	1023	67 21.8	49374
22	1987	3 08.5	18999	45593	18971	1041	67 22.7	49393
23	1988	3 12.4	18983	45626	18953	1062	67 24.6	49418
24	1989	3 15.9	18966	45662	18935	1080	67 26.6	49444
25	1990	3 18.8	18962	45684	18930	1096	67 27.5	49463
26	1991	3 22.2	18951	45709	18918	1114	67 28.8	49482
27	1992	3 25.3	18954	45726	18921	1131	67 29.1	49499
28	1993	3 29.8	18956	45744	18921	1156	67 29.4	49516
29	1994	3 34.8	18954	45772	18917	1183	67 30.4	49541
30	1995	3 39.8	18959	45797	18921	1212	67 30.7	49566
31	1996	3 45.0	18966	45822	18925	1241	67 30.9	49592
32	1997	3 50.9	18963	45857	18920	1273	67 32.0	49623
33	1998	3 57.3	18956	45897	18911	1308	67 33.6	49658
34	1999	4 02.5	18958	45931	18911	1336	67 34.3	49689
35	2000	4 07.8	18955	45969	18906	1365	67 35.5	49724
36	2001	4 13.0	18962	46005	18911	1394	67 36.0	49760
37	2002	4 18.4	18969	46044	18916	1424	67 36.6	49798
38	2003	4 24.2	18970	46090	18914	1457	67 37.7	49841
39	2004	4 29.4	18980	46121	18922	1486	67 37.9	49874
40	2005	4 34.7	18984	46155	18924	1515	67 38.5	49906
41	2006	4 39.8	18997	46177	18934	1544	67 38.3	49932
42	2007	4 45.8	19007	46207	18942	1578	67 38.4	49963
43	2008	4 52.5	19014	46236	18945	1616	67 38.7	49993
44	2009	4 59.7	19022	46264	18950	1656	67 39.0	50022
45	2010	5 08.0	19018	46301	18941	1701	67 40.2	50055
46	2011	5 16.1	19015	46338	18935	1746	67 41.3	50088
47	2012	5 24.6	19014	46377	18929	1793	67 42.4	50123
48	2013	5 32.8	19020	46411	18931	1838	67 42.9	50157
49	2014	5 40.3	19025	46446	18932	1880	67 43.5	50191
50	2015	5 48.8	19019	46495	18922	1926	67 45.1	50235
51	2016	5 57.2	19027	46538	18924	1974	67 45.8	50277
52	2017	6 06.4	19026	46592	18918	2024	67 47.2	50327
53	2018	6 15.5	19032	46648	18918	2075	67 48.3	50381
54	2019	6 24.9	19033	46712	18914	2127	67 49.9	50441
55	2020	6 33.4	19029	46775	18905	2173	67 51.7	50497
56	2021	6 41.3	19024	46840	18894	2216	67 53.8	50556
57	2022	6 49.5	19015	46907	18880	2260	67 56.0	50614

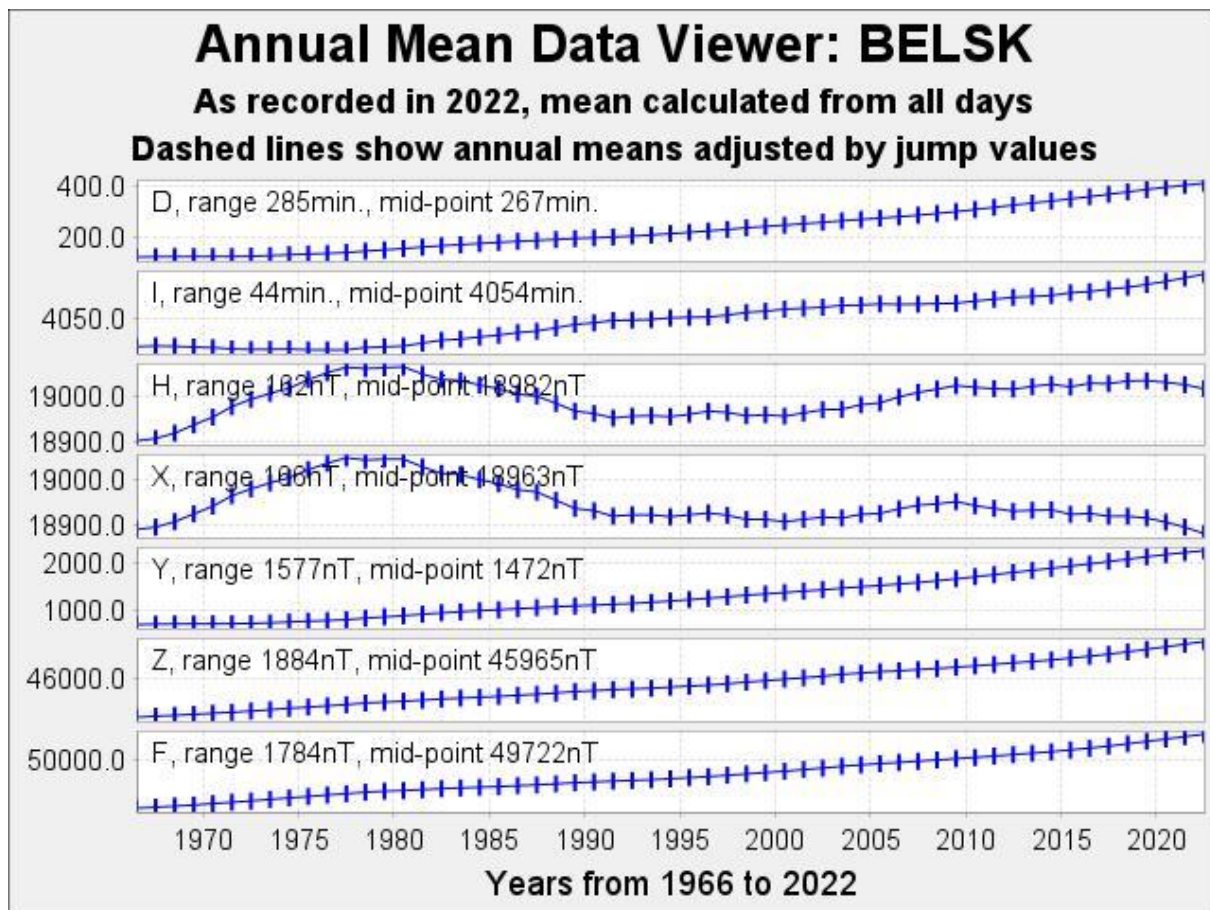


Fig. 7. Secular changes of H , X , Y , Z , F , D and I at Belsk.

Table 7
Monthly and yearly mean values of magnetic components
BEL 2022

	Jan	Feb	Mar	Apr	May	Jun	Jul	Aug	Sep	Oct	Nov	Dec	Mean
North component: 18500 + ... in nT													
All days	383	382	383	382	389	388	384	382	376	372	373	369	380
Quiet days	389	386	386	386	391	388	384	386	383	379	383	378	385
Disturbed days	372	371	377	372	386	386	382	374	363	363	364	357	372
East component: 2000 + ... in nT													
All days	240	243	246	250	254	257	262	265	268	272	275	279	259
Quiet days	236	242	246	250	253	256	262	264	267	270	272	277	258
Disturbed days	245	245	246	254	258	259	269	266	272	273	281	281	262
Vertical component: 46500 + ... in nT													
All days	380	386	389	394	395	402	407	412	418	426	432	439	407
Quiet days	377	385	388	392	394	400	408	410	416	424	429	435	405
Disturbed days	384	388	392	397	399	406	410	415	420	428	433	442	409

Table 8
 Three-hour-range K indices
 Belsk, January–March 2022
 The limit of $K = 9$ is 450

Day	January		February		March	
	K	SK	K	SK	K	SK
1	2421 2342	20	1111 2113	11	*232 2232	*
2	3112 1334	18	4211 2421	17	1112 1111	9
3	2332 2233	20	2445 4343	29	1111 1233	13
4	2311 1010	9	4333 3654	31	3222 1234	19
5	1210 1210	8	2222 3341	19	3223 4456	29
6	0000 0110	2	4233 3243	24	4243 3223	23
7	0000 0000	0	2212 1322	15	3212 3232	18
8	0002 1266	17	1111 1232	12	3211 1133	15
9	3222 2223	18	1111 1112	9	3112 1113	13
10	2211 2341	16	3223 3555	28	2112 1343	17
11	11*2 1310	*	3324 2354	26	4332 3345	27
12	1111 1121	9	3322 3344	24	5422 1123	20
13	1101 0121	7	4223 3433	24	1014 5656	28
14	0012 2356	19	2222 2321	16	5212 2212	17
15	5222 3454	27	1111 1110	7	1111 2324	15
16	3322 2353	23	1112 2443	18	0112 2332	14
17	3112 2333	18	2121 1122	12	2212 1101	10
18	5332 3433	26	0112 2233	14	3000 1120	7
19	5533 3333	28	2211 2323	16	1122 0022	10
20	3111 1111	10	4332 1242	21	2321 1203	14
21	1011 3344	17	1122 4243	19	3011 1112	10
22	2221 3334	20	3333 213*	*	2221 2242	17
23	3222 1211	14	*121 2323	*	2121 2221	13
24	1111 2123	12	3231 1112	14	3323 3211	18
25	2232 3334	22	2223 2112	15	3212 2220	14
26	2223 2334	21	0011 0011	4	3112 1232	15
27	1111 2243	15	1133 3431	19	2223 3554	26
28	1212 1125	15	1222 223*	*	3311 1112	13
29	4323 4111	19			1122 2433	18
30	3222 2224	19			1112 1334	16
31	3222 *322	*			4444 5523	31

Table 9
 Three-hour-range K indices
 Belsk, April–June 2022
 The limit of $K = 9$ is 450

Day	April		May		June	
	K	SK	K	SK	K	SK
1	3323 4222	21	3222 2222	17	1222 1211	12
2	4432 2353	26	3110 1222	12	0112 2222	12
3	3122 2332	18	2111 2212	12	1111 2212	11
4	4323 2230	19	1121 2123	13	0111 1120	7
5	1222 2222	15	1111 1221	10	0112 2221	11
6	3112 1211	12	0121 1321	11	1114 3333	19
7	1322 2323	18	0011 2102	7	2212 1212	13
8	3211 2232	16	1112 3222	14	2112 1131	12
9	3333 3341	23	2222 2221	15	1122 2212	13
10	2643 2234	26	0001 2211	7	2112 2211	12
11	3322 2221	17	2101 2232	13	3232 2322	19
12	2113 3443	21	2111 3432	17	2223 3432	21
13	3231 2112	15	21*3 2233	*	3422 3322	21
14	3334 4654	32	2212 2332	17	2222 2223	17
15	4434 4423	28	3422 3322	21	2333 4532	25
16	2222 3222	17	2333 3331	21	1222 4224	19
17	2222 3323	19	1333 4332	22	3333 3332	23
18	1223 1332	17	3212 1222	15	3223 1335	22
19	3112 2211	13	3332 3223	21	4323 3321	21
20	3122 1224	17	2323 3423	22	2223 4431	21
21	2222 3231	17	3322 3431	21	2223 2223	18
22	1212 2221	13	4332 2221	19	2232 3232	19
23	2113 3343	20	2222 1100	10	2233 2232	19
24	2221 1221	13	1212 3111	12	3111 1233	15
25	0122 1231	12	1222 1221	13	3222 2434	22
26	0011 2211	8	1111 2221	11	4234 4343	27
27	1221 5434	22	0113 5534	22	4422 1022	17
28	3332 3333	23	5443 3322	26	1222 2*24	*
29	3323 3232	21	3323 3433	24	2122 2111	12
30	4323 3323	23	3222 1333	19	1111 2111	9
31			3212 3332	19		

Table 10
 Three-hour-range K indices
 Belsk, July–September 2022
 The limit of $K = 9$ is 450

Day	July		August		September	
	K	SK	K	SK	K	SK
1	1101 2234	14	4222 3222	19	3333 2231	20
2	4542 2313	24	2223 2333	20	1123 2115	16
3	2012 3233	16	2222 2332	18	5333 3344	28
4	3334 3443	27	2222 3332	19	4455 4655	38
5	0111 1221	9	3211 2212	14	4344 4545	33
6	1122 2210	11	1012 1112	9	4333 3444	28
7	0123 5333	20	2223 4445	26	3233 3431	22
8	4433 3332	25	4444 3344	30	2333 333*	*
9	1112 4312	15	3334 4433	27	4123 3212	18
10	1232 3221	16	2313 3443	23	3232 3442	23
11	1113 3453	21	2213 3554	25	2222 2432	19
12	3344 4332	26	3122 2211	14	2222 1131	14
13	1112 2220	11	1222 3332	18	0111 1101	6
14	1111 2221	11	3222 2210	14	1122 2234	17
15	2212 3333	19	1122 3311	14	4121 1311	14
16	2232 1111	13	1111 1112	9	0123 1111	10
17	1121 1121	10	2313 3554	26	1112 2112	11
18	1123 3233	18	3333 5555	32	2223 3322	19
19	3444 5354	32	3323 3454	27	3212 3323	19
20	2212 2222	15	4222 0144	19	2222 2132	16
21	2123 4653	26	3323 3432	23	2122 2101	11
22	3333 2322	21	3222 1221	15	0111 2224	13
23	4532 2123	22	1111 1122	10	2132 3423	20
24	3232 2231	18	1112 1201	9	2323 3443	24
25	2212 2222	15	1122 2112	12	1122 2202	12
26	3213 2212	16	0111 2122	10	2102 1113	11
27	2323 3323	21	2114 5333	22	5434 3224	27
28	2222 3221	16	2224 2221	17	111* 1222	*
29	1111 2222	12	2333 4231	21	1122 2222	14
30	2212 3323	18	2324 2233	21	2333 3211	18
31	2212 3423	19	3312 2325	21		

Table 11
 Three-hour-range K indices
 Belsk, October–December 2022
 The limit of $K = 9$ is 450

Day	October		November		December	
	K	SK	K	SK	K	SK
1	1001 1211	7	1123 2132	15	3433 4544	30
2	2112 2425	19	2222 2443	21	2333 3343	24
3	4232 4463	28	3124 4534	26	1322 2322	17
4	2242 1254	22	3333 2333	23	2212 3654	25
5	3322 2344	23	3322 3212	18	0221 3221	13
6	2222 3444	23	1011 0111	6	0111 2121	9
7	4333 3321	22	1123 3551	21	1112 5543	22
8	1222 3342	19	2222 3222	17	2222 2224	18
9	4333 3554	30	3211 1100	9	4223 2222	19
10	2323 2223	19	0011 1110	5	3213 1332	18
11	3121 1123	14	0122 2323	15	2212 3324	19
12	2121 2242	16	3221 1101	11	2111 1223	13
13	1110 1123	10	1321 2321	15	2111 1111	9
14	2133 3323	20	0022 1131	10	0110 1322	10
15	5223 2352	24	1111 1111	8	1221 1311	12
16	3233 4334	25	0011 1221	8	2111 1121	10
17	1111 1411	11	0111 1001	5	2101 1000	5
18	0122 1223	13	1012 2243	15	0011 1122	8
19	2112 1112	11	2012 2111	10	2321 2233	18
20	1112 3223	15	1011 1333	13	1111 1232	12
21	1112 1122	11	3322 2222	18	2132 2422	18
22	2223 4653	27	1111 1210	8	1111 3453	19
23	2222 2454	23	0110 1121	7	4233 5435	29
24	3222 2112	15	1121 2133	14	3433 3533	27
25	0012 1211	8	3333 3354	27	3211 2223	16
26	0011 1233	11	4232 4343	25	3233 6521	25
27	2223 3332	20	2322 4353	24	4433 4533	29
28	2222 3534	23	4532 1254	26	2221 2122	14
29	3344 4444	30	4333 4543	29	1112 3434	19
30	2223 2342	20	3334 4364	30	4333 4554	31
31	3322 2432	21			3222 3344	23

Table 12
 Three-hour-range *E* indices
 based on power spectrum estimation (*)
 Belsk, January–March 2022

Day	January		February		March	
	<i>E</i>	<i>SE</i>	<i>E</i>	<i>SE</i>	<i>E</i>	<i>SE</i>
1	2421 1441	19	1111 2013	10	*222 2242	*
2	3112 1335	19	5211 2421	18	1112 1101	8
3	2433 1234	22	2555 5443	33	0000 1233	9
4	1311 0000	6	4433 4654	33	4222 1335	22
5	0200 1200	5	3212 3352	21	4214 5556	32
6	0000 0000	0	4233 4243	25	5253 3233	26
7	0000 0000	0	2212 1333	17	4212 3231	18
8	0001 1276	17	1111 1232	12	3211 1132	14
9	3221 2223	17	1001 0002	4	3011 1103	10
10	2210 1341	14	4222 2565	28	2111 1443	17
11	11*1 1310	*	4224 1365	27	4342 3345	28
12	0100 1121	6	4332 3454	28	5531 1023	20
13	1001 0021	5	4323 4544	29	1004 5566	27
14	0012 2256	18	2122 2321	15	5212 2212	17
15	5222 3555	29	1101 1100	5	1110 2224	13
16	4323 3463	28	1112 2453	19	0011 2332	12
17	3112 2443	20	2121 1022	11	2212 0101	9
18	6332 3443	28	0012 2234	14	3000 0020	5
19	5543 3343	30	3211 2423	18	1022 0022	9
20	3010 0101	6	5221 1241	18	2321 1104	14
21	0011 2355	17	0022 5254	20	3010 1102	8
22	3321 3434	23	3433 103*	*	2221 2252	18
23	4312 1200	13	*022 2333	*	2121 2221	13
24	0011 2013	8	3321 0002	11	4312 3212	18
25	2223 3335	23	3233 2101	15	3212 2220	14
26	1223 2334	20	0011 0010	3	3001 0242	12
27	0011 2253	14	0133 2421	16	2224 3554	27
28	1211 1035	14	1213 213*	*	3311 1011	11
29	3333 4011	18			1022 2434	18
30	3232 3224	21			0012 1235	14
31	3213 *323	*			5444 5422	30

*) see Reda and Jankowski (2004)

Table 13
 Three-hour-range E indices
 based on power spectrum estimation (*)
 Belsk, April–June 2022

Day	April		May		June	
	E	SE	E	SE	E	SE
1	3324 3233	23	3222 1221	15	1122 1211	11
2	4532 2353	27	3100 0231	10	0112 2213	12
3	3012 2432	17	1111 2113	11	1111 1112	9
4	4422 2240	20	1122 2124	15	0011 1120	6
5	1213 2221	14	0111 1221	9	0002 2221	9
6	3112 1311	13	0121 1321	11	1115 3334	21
7	1422 3323	20	0001 1101	4	2312 2212	15
8	4211 2122	15	1112 3222	14	2112 1131	12
9	4333 4451	27	3222 2211	15	1112 2112	11
10	2653 2334	28	0000 1211	5	2103 2111	11
11	3323 1231	18	2100 1232	11	3222 2322	18
12	3002 4553	22	2111 3422	16	2223 3432	21
13	3231 1000	10	21*3 2233	*	3421 2422	20
14	3434 4665	35	2112 2333	17	2222 2323	18
15	5434 4423	29	3422 3321	20	2444 5422	27
16	1211 3323	16	2323 3321	19	1223 4225	21
17	2222 3423	20	1333 4342	23	3334 4342	26
18	1223 1342	18	4112 1212	14	3223 1235	21
19	3112 2110	11	3332 3233	22	5223 3420	21
20	4122 1224	18	2333 2424	23	2123 4431	20
21	2222 3231	17	3322 3521	21	2213 2223	17
22	1212 2221	13	5433 2221	22	2222 3233	19
23	2113 3344	21	2122 1100	9	2233 2232	19
24	2111 1220	10	0201 3011	8	3100 1243	14
25	0022 1231	11	1222 1221	13	3223 3445	26
26	0001 2110	5	0111 2211	9	5224 5454	31
27	1111 5544	22	0003 5534	20	4421 1022	16
28	4342 2344	26	5444 2212	24	1222 2*25	*
29	4423 3342	25	4333 3434	27	2122 2100	10
30	4333 2323	23	3222 1233	18	1101 1101	6
31			3312 3232	19		

*) see Reda and Jankowski (2004)

Table 14
 Three-hour-range E indices
 based on power spectrum estimation (*)
 Belsk, July–September 2022

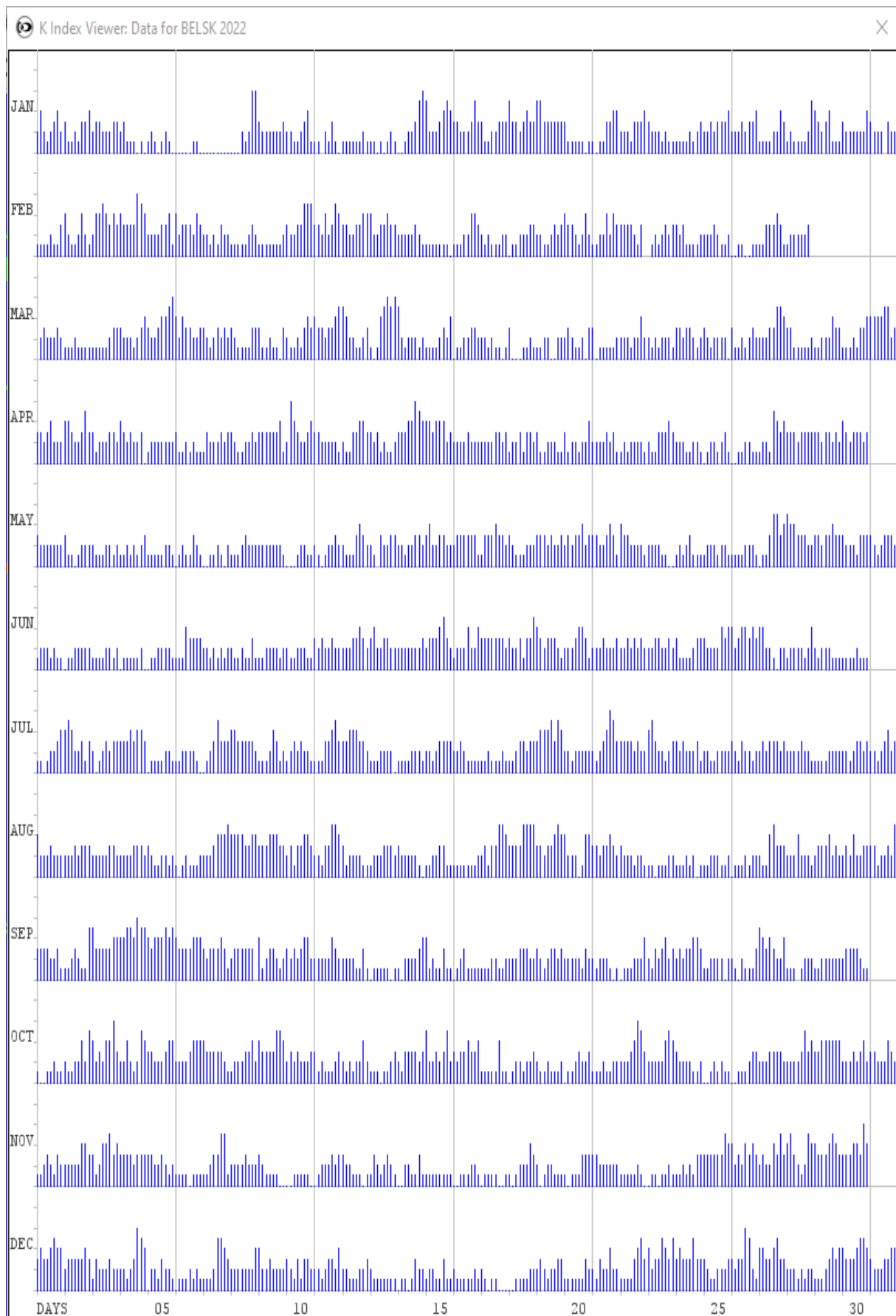
Day	July		August		September	
	E	SE	E	SE	E	SE
1	1101 1134	12	4222 3123	19	3433 1131	19
2	4542 2303	23	2223 2333	20	1123 2125	17
3	2013 3243	18	3222 2242	19	6333 4345	31
4	3434 3553	30	1221 3422	17	5565 4655	41
5	0011 1210	6	3211 1202	12	5444 4655	37
6	1022 1210	9	1001 1011	5	4423 2554	29
7	0023 5434	21	1223 5545	27	3233 4431	23
8	4434 3232	25	4444 3345	31	3444 343*	*
9	1111 4312	14	3434 4443	29	5123 3203	19
10	0132 3221	14	1313 3453	23	3233 3442	24
11	0113 2453	19	2213 3554	25	2113 2533	20
12	4344 5343	30	2132 2211	14	3221 1131	14
13	1012 2120	9	1232 3433	21	0111 1100	5
14	0111 1221	9	3212 2100	11	1022 2234	16
15	2202 3333	18	1111 3300	10	4011 1211	11
16	2332 1111	14	1011 1103	8	0112 1200	7
17	1111 1121	9	2213 3655	27	0102 2113	10
18	1123 4133	18	3333 5555	32	2213 4332	20
19	3554 5354	34	4323 3565	31	3112 3434	21
20	2212 2222	15	4231 0045	19	2212 2242	17
21	3124 4644	28	4223 3532	24	2022 1100	8
22	3332 2322	20	3312 1221	15	0111 2234	14
23	3532 2124	22	0100 1112	6	2132 3424	21
24	3232 2331	19	0111 1100	5	2323 3443	24
25	2211 2222	14	1112 2002	9	0121 1103	9
26	4213 3213	19	0111 2122	10	2002 1014	10
27	3323 3333	23	2014 5344	23	6435 3224	29
28	2221 3221	15	2224 2221	17	110* 0132	*
29	1101 1222	10	1333 3231	19	1122 2212	13
30	2112 3323	17	2433 2234	23	3333 4211	20
31	2113 4523	21	3312 2325	21		

*) see Reda and Jankowski (2004)

Table 15
 Three-hour-range E indices
 based on power spectrum estimation (*)
 Belsk, October–December 2022

Day	October		November		December	
	E	SE	E	SE	E	SE
1	0001 1211	6	1033 2032	14	3534 5644	34
2	2122 2426	21	2222 3553	24	3333 3452	26
3	5332 4463	30	3134 5545	30	1323 1432	19
4	3352 1264	26	4333 3434	27	2212 4665	28
5	3332 2455	27	3423 3212	20	0121 3220	11
6	2222 4565	28	0010 0011	3	0101 1110	5
7	5433 3310	22	0113 4551	20	1102 5543	21
8	1333 3341	21	2333 3232	21	2222 1124	16
9	4433 4554	32	3311 1000	9	4223 1112	16
10	2313 1234	19	0000 0000	0	3213 1342	19
11	3111 1124	14	0122 2323	15	2221 2424	19
12	1011 2143	13	3221 0000	8	2111 1223	13
13	1110 1023	9	1321 2321	15	1001 1101	5
14	2234 4213	21	0011 1130	7	0110 1332	11
15	5323 1452	25	0010 0000	1	1111 1321	11
16	3234 4324	25	0001 0221	6	3101 1121	10
17	1101 1400	8	0000 1001	2	1100 0000	2
18	0012 1323	12	1011 2254	16	0011 0112	6
19	2112 1012	10	2002 1001	6	2421 2233	19
20	0012 4224	15	0001 1344	13	1011 0132	9
21	0112 0122	9	3322 2212	17	3132 2422	19
22	2123 4653	26	1101 1210	7	1011 4453	19
23	2112 2564	23	0010 1120	5	5132 5536	30
24	3222 2012	14	0111 1124	11	3544 3644	33
25	0012 1300	7	2233 3455	27	3211 2223	16
26	0011 1233	11	4332 4353	27	3234 5521	25
27	2213 3421	18	3312 4353	24	5433 4632	30
28	2222 3545	25	5522 1264	27	2211 1011	9
29	4445 4445	34	5333 5553	32	0013 3545	21
30	2323 2442	22	3324 4364	29	5443 5654	36
31	1332 2532	21			3222 4455	27

^{*)} see Reda and Jankowski (2004)

Fig. 8. *K*-indices in graphical form, Belsk 2022.

8. TABLES AND PLOTS FOR HEL OBSERVATORY

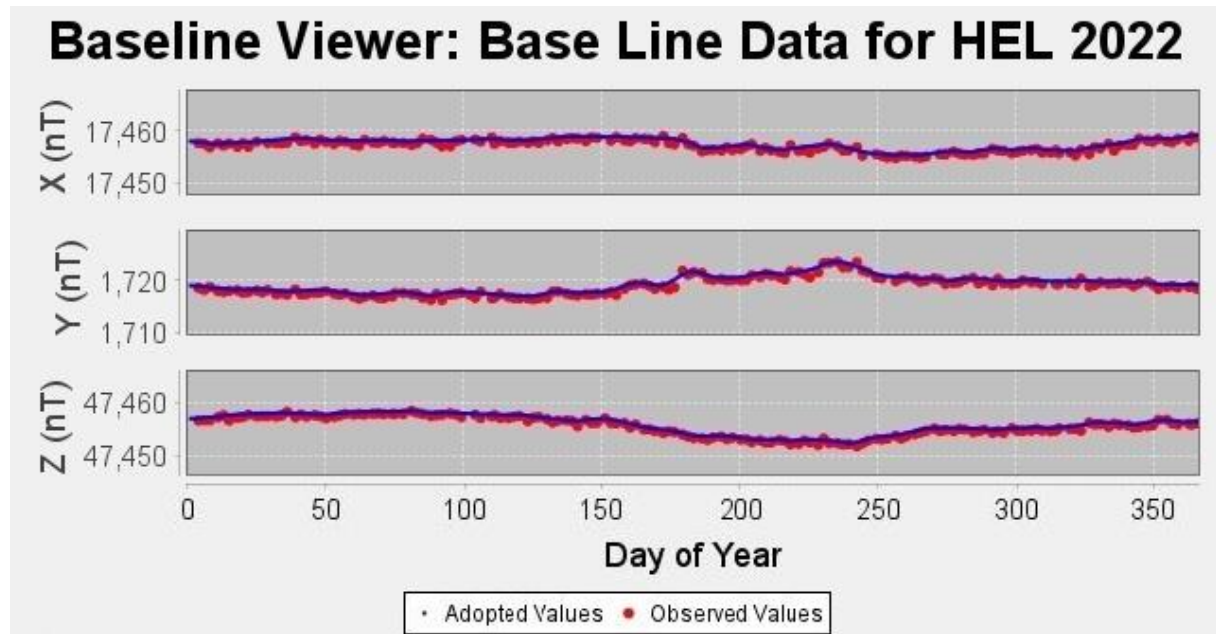


Fig. 9. Base values of set 1, Hel 2022.

Table 16
Annual mean values of magnetic components in Hel Observatory

No.	Year	D [° ']	H [nT]	Z [nT]	X [nT]	Y [nT]	I [° ']	F [nT]
1	1953	-0 14.5	17388	45327	17388	-73	69 00.8	48548
2	1954	-0 10.0	17394	45374	17394	-51	69 01.5	48594
3	1955	-0 04.2	17379	45430	17379	-21	69 03.9	48640
4	1956	0 03.9	17371	45450	17371	20	69 05.0	48656
5	1957	0 05.7	17372	45475	17372	29	69 05.5	48680
6	1958	0 10.2	17380	45535	17380	52	69 06.5	48739
7	1959	0 14.7	17390	45565	17390	74	69 06.6	48771
8	1960	0 17.6	17402	45602	17402	89	69 06.8	48810
9	1961	0 19.8	17422	45625	17422	100	69 06.0	48838
10	1962	0 22.7	17438	45647	17438	115	69 05.5	48864
11	1963	0 26.5	17449	45663	17448	134	69 05.2	48883
12	1964	0 28.6	17464	45676	17463	145	69 04.6	48901
13	1965	0 30.0	17476	45692	17475	152	69 04.2	48920
14	1966	0 31.6	17485	45710	17484	161	69 04.0	48940
15	1967	0 33.3	17492	45743	17491	169	69 04.4	48973
16	1968	0 34.4	17502	45769	17501	175	69 04.4	49001
17	1969	0 34.3	17524	45792	17523	175	69 03.5	49030
18	1970	0 34.8	17542	45824	17541	178	69 03.2	49067
19	1971	0 35.7	17565	45849	17564	182	69 02.3	49098
20	1972	0 36.1	17579	45880	17578	184	69 02.1	49132

to be continued

Table 16 (continuation)
Annual mean values of magnetic components in Hel Observatory

No.	Year	D [° ']	H [nT]	Z [nT]	X [nT]	Y [nT]	I [° ']	F [nT]
21	1973	0 38.5	17595	45912	17594	197	69 01.9	49168
22	1974	0 41.9	17606	45951	17605	215	69 02.2	49208
23	1975	0 45.0	17625	45984	17623	231	69 01.7	49246
24	1976	0 49.6	17639	46015	17637	254	69 01.6	49280
25	1977	0 55.0	17651	46045	17649	282	69 01.5	49312
26	1978	1 00.2	17646	46085	17643	309	69 02.9	49349
27	1979	1 05.1	17651	46112	17648	334	69 03.2	49375
28	1980	1 11.5	17653	46127	17649	367	69 03.5	49390
29	1981	1 17.5	17637	46156	17632	398	69 05.2	49411
30	1982	1 23.4	17620	46184	17615	427	69 07.1	49431
31	1983	1 28.6	17614	46200	17608	454	69 07.8	49444
32	1984	1 33.5	17602	46219	17596	479	69 09.1	49457
33	1985	1 37.9	17591	46239	17584	501	69 10.3	49472
34	1986	1 42.7	17579	46263	17571	525	69 11.6	49490
35	1987	1 46.3	17572	46285	17564	543	69 12.6	49508
36	1988	1 51.0	17555	46318	17546	567	69 14.6	49533
37	1989	1 55.5	17535	46352	17525	589	69 16.7	49558
38	1990	1 58.4	17527	46374	17516	604	69 17.8	49575
39	1991	2 00.6	17513	46398	17502	614	69 19.3	49593
40	1992	2 03.9	17515	46416	17504	631	69 19.6	49611
41	1993	2 10.0	17516	46428	17503	662	69 19.8	49622
42	1994	2 15.9	17512	46456	17498	692	69 20.7	49647
43	1995	2 21.3	17518	46481	17503	720	69 21.0	49672
44	1996	2 26.6	17523	46506	17507	747	69 21.2	49698
45	1997	2 32.9	17519	46539	17502	779	69 22.3	49727
46	1998	2 39.8	17512	46581	17493	814	69 23.8	49764
47	1999	2 45.4	17511	46615	17491	842	69 24.7	49796
48	2000	2 51.9	17507	46657	17485	875	69 25.9	49833
49	2001	2 57.7	17515	46692	17492	905	69 26.2	49869
50	2002	3 03.7	17520	46730	17495	936	69 26.9	49906
51	2003	3 10.8	17519	46777	17492	972	69 28.1	49950
52	2004	3 16.6	17529	46809	17500	1002	69 28.2	49983
53	2005	3 22.3	17531	46843	17501	1031	69 28.9	50016
J	2006.0	0 -1.5	-2	9	-2	-8	0 0.6	7
54	2006	3 29.9	17550	46859	17517	1071	69 28.1	50038
55	2007	3 36.7	17559	46887	17524	1106	69 28.2	50067
56	2008	3 43.8	17564	46917	17527	1143	69 28.5	50097
57	2009	3 51.3	17571	46945	17531	1181	69 28.8	50126
58	2010	4 00.5	17568	46980	17525	1228	69 29.8	50157
59	2011	4 09.2	17564	47014	17518	1272	69 30.9	50188

to be continued

Table 16 (continuation)
Annual mean values of magnetic components in Hel Observatory

No.	Year	D [° ']	H [nT]	Z [nT]	X [nT]	Y [nT]	I [° ']	F [nT]
60	2012	4 18.7	17562	47053	17512	1321	69 32.0	50223
61	2013	4 28.2	17567	47084	17513	1369	69 32.4	50254
62	2014	4 36.3	17571	47117	17514	1411	69 32.9	50286
63	2015	4 45.5	17565	47163	17504	1457	69 34.4	50328
64	2016	4 54.7	17569	47203	17504	1504	69 35.1	50367
65	2017	5 05.5	17567	47253	17498	1559	69 36.4	50413
66	2018	5 15.7	17570	47305	17496	1611	69 37.4	50463
J	2019.0	0 –0.2	5	–2	5	–1	0 –0.4	0
67	2019	5 26.1	17564	47366	17485	1664	69 39.3	50518
68	2020	5 35.6	17560	47425	17477	1712	69 40.9	50571
69	2021	5 44.7	17553	47487	17464	1757	69 42.9	50627
70	2022	5 53.7	17543	47550	17450	1802	69 45.0	50683

Note: Since 2006 the observatory has stopped introducing the so-called historical corrections. The corrections were related, among other things, with the variable location of the instruments for absolute measurements. In the 2006.0 line we include the jump value *J* relating to the neglect of historical corrections. The jump values are defined as follows:

jump value *J* = old site value – new site value

2019.0 – jump caused by change the method for measuring declination/inclination from residual to zero method.

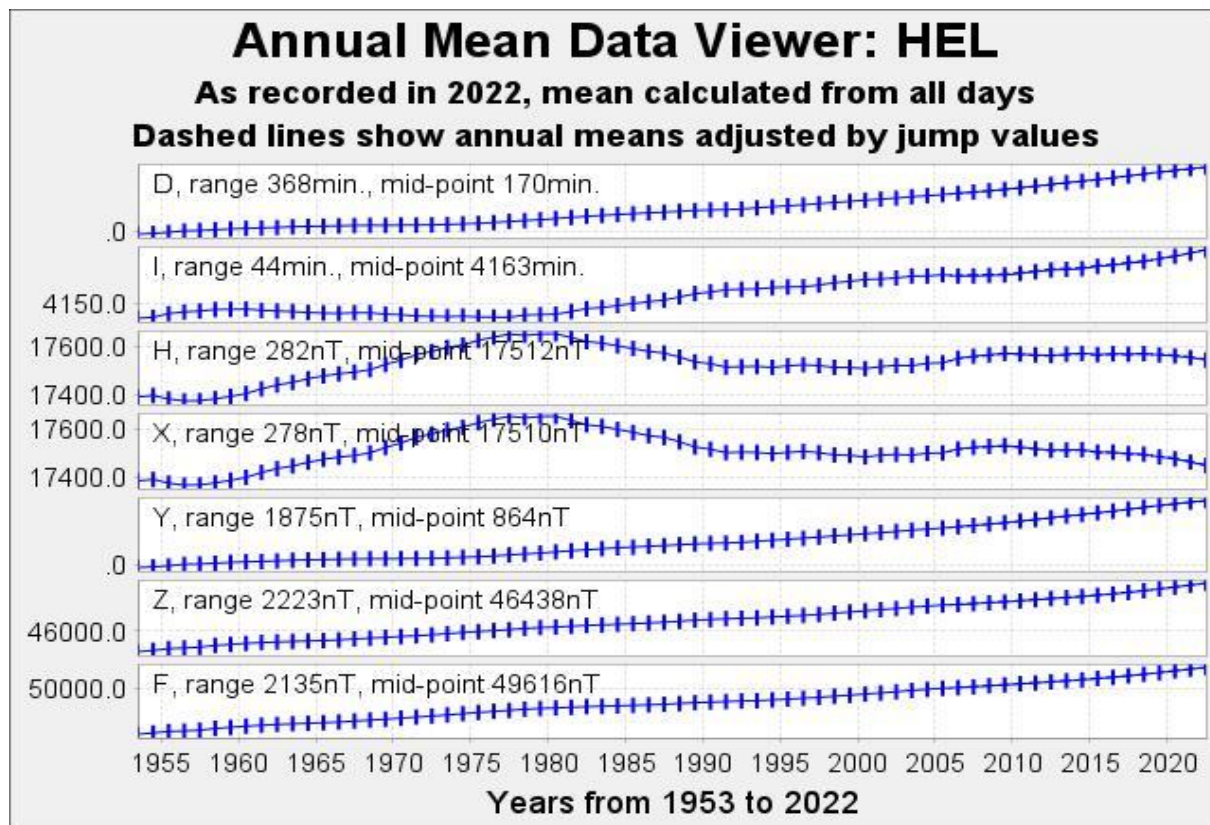


Fig. 10. Secular changes of *H*, *X*, *Y*, *Z*, *F*, *D* and *I* at Hel.

Table 17
Monthly and yearly mean values of magnetic components
HLP 2022

	Jan	Feb	Mar	Apr	May	Jun	Jul	Aug	Sep	Oct	Nov	Dec	Mean
North component: 17000 + ... in nT													
All days	452	451	452	452	459	459	456	452	445	442	442	439	450
Quiet days	458	454	455	456	461	458	455	456	451	448	451	448	454
Disturbed days	442	440	447	442	457	459	454	446	433	434	433	427	443
East component: 1500 + ... in nT													
All days	284	287	289	292	295	298	304	306	310	315	319	323	302
Quiet days	280	286	288	292	294	297	303	305	309	314	317	321	300
Disturbed days	290	289	288	296	298	300	310	307	314	316	325	324	305
Vertical component: 47000 + ... in nT													
All days	525	531	534	537	538	544	550	554	561	569	575	582	550
Quiet days	523	530	533	536	537	542	551	552	560	566	572	578	548
Disturbed days	529	533	537	540	542	549	553	557	561	571	575	585	553

Table 18
 Three-hour-range K indices
 Hel, January–March 2022
 The limit of $K = 9$ is 550

Day	January		February		March	
	K	SK	K	SK	K	SK
1	3422 2442	23	2111 2114	13	2133 3232	19
2	3112 1334	18	5211 2421	18	1112 1111	9
3	2433 2234	23	2545 4343	30	1011 2233	13
4	2311 1011	10	4433 4654	33	3222 2334	21
5	1200 1200	6	3222 3342	21	3224 4466	31
6	0000 0000	0	4233 4243	25	4243 3233	24
7	0000 0000	0	2212 1323	16	3212 3332	19
8	0012 1266	18	2111 1232	13	3211 1033	14
9	3222 2223	18	1101 0002	5	3111 1103	11
10	2211 2342	17	3223 3555	28	2112 2343	18
11	1101 1310	8	4324 2364	28	4442 3345	29
12	1110 1121	8	3332 3344	25	5432 1123	21
13	1001 0021	5	4323 3444	27	2014 5556	28
14	0012 2356	19	2122 2321	15	5223 3312	21
15	5222 3454	27	2111 1211	10	1211 3324	17
16	3333 2353	25	1112 3443	19	0012 3332	14
17	2113 2333	18	2112 2022	12	2212 1101	10
18	5233 3433	26	0022 2233	14	3101 1121	10
19	5533 3333	28	2212 2323	17	1122 0022	10
20	3110 0101	7	4332 1242	21	2312 2203	15
21	0011 3344	16	1122 4243	19	3011 1212	11
22	3221 3333	20	3333 2132	20	2221 3242	18
23	3312 1111	13	1122 3333	18	3122 2221	15
24	0011 2123	10	3331 1112	15	4323 3212	20
25	2232 3334	22	3223 2111	15	3212 2220	14
26	2223 2334	21	0011 0011	4	3102 1232	14
27	1112 2243	16	1133 3431	19	2224 3554	27
28	2212 1125	16	2223 2232	18	3412 1112	15
29	4423 4011	19			1112 2433	17
30	3222 3224	20			1112 1234	15
31	3222 2323	19			5444 5533	33

Table 19
 Three-hour-range K indices
 Hel, April–June 2022
 The limit of $K = 9$ is 550

Day	April		May		June	
	K	SK	K	SK	K	SK
1	3223 4233	22	3322 2222	18	2222 2212	15
2	4443 3353	29	3111 1232	14	0012 2223	12
3	3122 2333	19	2111 2213	13	1111 2113	11
4	4333 2330	21	1222 2113	14	0011 1120	6
5	1223 3222	17	0111 1222	10	0112 2231	12
6	3122 1212	14	0121 1221	10	1114 3333	19
7	2322 3323	20	0001 2102	6	2213 1213	15
8	3222 2233	19	2113 3222	16	2112 0131	11
9	3333 4441	25	3232 2221	17	1122 2212	13
10	2653 3334	29	0001 2211	7	2213 3111	14
11	3323 2221	18	2101 2333	15	2233 3322	20
12	2103 4443	21	2211 4432	19	2223 3432	21
13	3232 2002	14	2113 2233	17	3522 3422	23
14	3334 5654	33	2212 2332	17	2322 2223	18
15	4434 4433	29	4433 3321	23	2343 5532	27
16	2222 3323	19	2334 3331	22	2223 4324	22
17	2222 3323	19	1333 4332	22	3334 4332	25
18	1223 1332	17	4212 1223	17	3223 2335	23
19	3113 3211	15	3332 3223	21	4323 3420	21
20	3133 1324	20	2333 3424	24	2223 4432	22
21	2232 3231	18	3322 3431	21	2223 3223	19
22	1213 2322	16	4333 3321	22	2223 3232	19
23	2213 4344	23	2223 1200	12	2233 2233	20
24	2222 2220	14	1202 3111	11	2111 2233	15
25	0122 2231	13	1222 1322	15	3222 3445	25
26	1011 2211	9	2112 3221	14	5234 5344	30
27	1222 5545	26	0123 5534	23	4422 2022	18
28	4332 3333	24	5444 3323	28	2222 3134	19
29	3333 3242	23	4323 4433	26	2222 3111	14
30	4333 3323	24	3223 2333	21	2111 2111	10
31			3212 3332	19		

Table 20
 Three-hour-range K indices
 Hel, July–September 2022
 The limit of $K = 9$ is 550

Day	July		August		September	
	K	SK	K	SK	K	SK
1	2101 2234	15	3323 3223	21	3433 2321	21
2	4443 2313	24	2333 2322	20	1223 3225	20
3	3013 3333	19	3223 2342	21	5333 3345	29
4	3434 4443	29	2222 3332	19	4555 4655	39
5	1111 1221	10	3211 2212	14	5444 4645	36
6	1023 2310	12	1112 2112	11	4333 3454	29
7	0023 6434	22	2224 4545	28	3233 3431	22
8	4534 4332	28	5444 3344	31	2333 3335	25
9	1111 4312	14	3334 4432	26	4123 3213	19
10	0233 3221	16	2323 4443	25	3233 3452	25
11	1023 3454	22	3224 4554	29	2223 3433	22
12	3244 5333	27	3122 2211	14	3222 2131	16
13	2012 2220	11	1223 3333	20	0111 1101	6
14	1111 2221	11	3222 2200	13	1122 2234	17
15	2202 3333	18	1222 3311	15	4011 2311	13
16	2233 1111	14	1112 2212	12	1223 2201	13
17	1122 2121	12	2423 4565	31	1112 2113	12
18	1223 3233	19	3334 5565	34	2223 4332	21
19	3444 5354	32	3323 3554	28	3213 3424	22
20	2212 3222	16	4222 1144	20	2222 2243	19
21	2223 4654	28	3333 3432	24	3122 2201	13
22	3333 2322	21	3223 2221	17	0121 3324	16
23	4533 2223	24	1101 1122	9	3133 3433	23
24	3222 2332	19	1112 2201	10	2324 3444	26
25	2112 2222	14	1112 2002	9	1122 2103	12
26	3213 3222	18	0112 2122	11	2103 2114	14
27	2323 3323	21	2014 5333	21	5434 4224	28
28	2222 3321	17	2224 2231	18	2110 1222	11
29	1101 2222	11	2334 4332	24	1122 3322	16
30	2222 4323	20	3334 3233	24	3343 4211	21
31	2223 4523	23	3312 3325	22		

Table 21
 Three-hour-range K indices
 Hel, October–December 2022
 The limit of $K = 9$ is 550

Day	October		November		December	
	K	SK	K	SK	K	SK
1	0001 1211	6	1123 2132	15	3443 4544	31
2	2123 3425	22	2222 2543	22	2333 3443	25
3	4233 4473	30	3134 4535	28	2333 2433	23
4	3343 2264	27	3333 2333	23	2212 3655	26
5	3333 2345	26	3323 3212	19	0222 3221	14
6	3232 3454	26	1011 0011	5	0111 1111	7
7	4333 3421	23	1123 4652	24	2012 5544	23
8	1333 4342	23	2322 3232	19	2222 2224	18
9	4334 4554	32	3311 1000	9	4223 2222	19
10	2323 2223	19	0000 0000	0	2223 1232	17
11	3121 2123	15	0122 2323	15	2212 2324	18
12	1111 2143	14	3222 1100	11	3111 1223	14
13	1110 2023	10	1321 2321	15	2111 1102	9
14	2133 4323	21	0022 1131	10	0110 1332	11
15	5333 2352	26	1111 1011	7	1221 1321	13
16	3234 4334	26	1001 0221	7	2101 2121	10
17	1111 2401	11	0100 1001	3	2100 1000	4
18	1122 1323	15	1011 2244	15	0101 1122	8
19	2112 1112	11	2012 2111	10	2321 2233	18
20	1012 4223	15	1010 1333	12	1111 1233	13
21	1112 1132	12	3323 2222	19	3132 3422	20
22	2123 4653	26	1101 1210	7	2112 4353	21
23	3222 2455	25	0011 2121	8	4233 5435	29
24	3222 2112	15	1111 2133	13	3433 3533	27
25	1012 1311	10	2333 3454	27	3211 2223	16
26	0011 1233	11	4332 4343	26	3233 6522	26
27	2223 3332	20	3322 4353	25	5444 4633	33
28	2222 3545	25	4532 2254	27	2222 1122	14
29	4344 4444	31	4323 4543	28	0013 3435	19
30	2223 2343	21	3325 4364	30	4333 4654	32
31	3332 2433	23			3232 3345	25

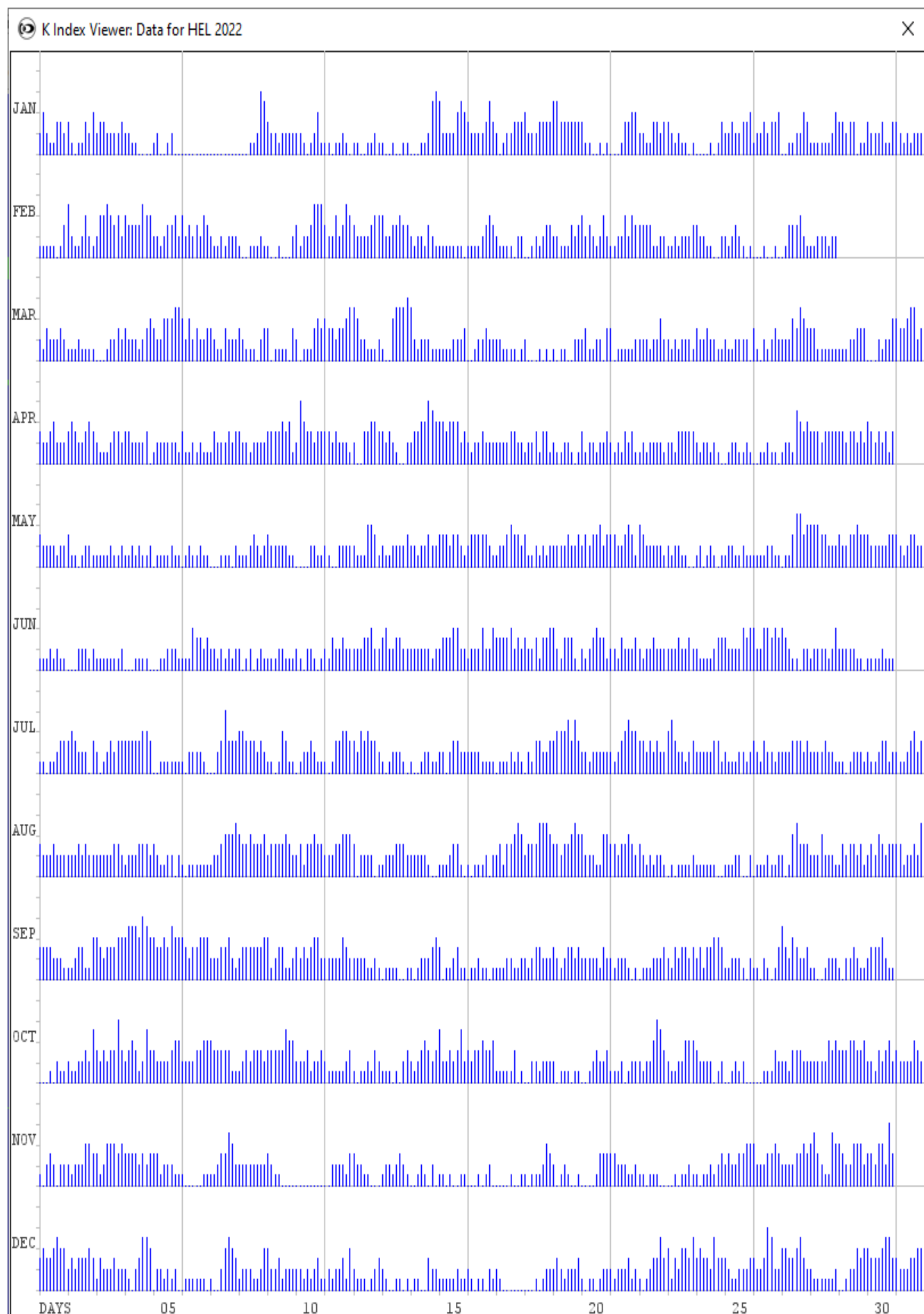


Fig. 11. *K*-indices in graphical form, Hel 2022.

9. TABLES AND PLOTS FOR HORNSUND OBSERVATORY

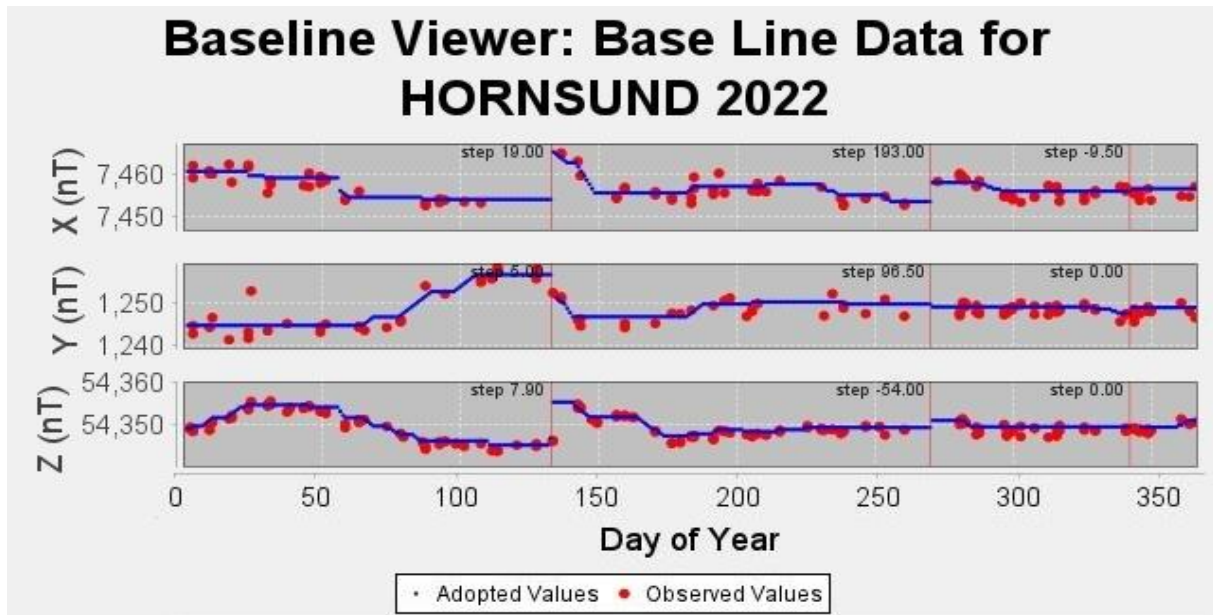


Fig. 12. Base values, Hornsund 2022.

Table 22
Annual mean values of magnetic components in Hornsund Observatory

No.	Year	D [° ']	H [nT]	Z [nT]	X [nT]	Y [nT]	I [° ']	F [nT]
1	1979	-0 32.2	8384	53447	8384	-79	81 05.1	54101
2	1980	-0 14.2	8370	53447	8370	-35	81 06.0	54098
3	1981	-0 09.3	8351	53449	8351	-23	81 07.2	54097
4	1982	-0 09.4	8319	53481	8319	-23	81 09.5	54124
5	1983	-0 02.0	8295	53457	8295	-5	81 10.8	54097
6	1984	0 07.7	8266	53439	8266	19	81 12.4	54075
7	1985	0 14.3	8238	53405	8238	34	81 13.9	54037
8	1986	0 20.4	8213	53392	8213	49	81 15.3	54020
9	1987	0 25.6	8193	53360	8193	61	81 16.3	53985
10	1988	0 34.7	8168	53368	8168	82	81 17.9	53989
11	1989	0 40.8	8148	53369	8147	97	81 19.2	53987
12	1990	0 47.2	8122	53360	8121	112	81 20.7	53975
13	1991	0 53.0	8107	53355	8106	125	81 21.6	53967
14	1992	1 01.4	8088	53352	8087	144	81 22.8	53962
15	1993	1 12.9	8065	53356	8063	171	81 24.3	53962
16	1994	1 25.9	8044	53374	8041	201	81 25.8	53977
17	1995	1 38.4	8038	53374	8035	230	81 26.1	53976
18	1996	1 51.4	8023	53385	8019	260	81 27.2	53985
19	1997	2 07.2	8004	53406	7999	296	81 28.6	54003
20	1998	2 24.0	8001	53440	7994	335	81 29.1	54036
21	1999	2 39.1	7998	53471	7989	370	81 29.6	54066
22	2000	2 55.5	7996	53504	7986	408	81 30.0	54098
23	2001	3 12.4	7992	53542	7979	447	81 30.6	54135
24	2002	3 29.7	7989	53585	7974	487	81 31.2	54177
25	2003	3 49.8	7965	53646	7947	532	81 33.3	54234
26	2004	4 04.2	7961	53675	7941	565	81 33.8	54262
27	2005	4 20.5	7953	53707	7930	602	81 34.6	54293
28	2006	4 36.2	7958	53727	7932	639	81 34.5	54314
29	2007	4 51.3	7950	53757	7922	673	81 35.2	54342
30	2008	5 07.9	7941	53785	7909	710	81 36.1	54368
31	2009	5 25.4	7939	53804	7903	750	81 36.4	54387
32	2010	5 45.7	7928	53837	7888	796	81 37.4	54418
33	2011	6 05.8	7920	53868	7875	841	81 38.2	54447
34	2012	6 28.2	7910	53900	7860	891	81 39.1	54477
35	2013	6 50.8	7903	53920	7846	942	81 39.7	54497
36	2014	7 08.8	7895	53947	7833	982	81 40.4	54521
37	2015	7 30.6	7881	53988	7813	1030	81 41.7	54560
38	2016	7 53.5	7862	54021	7787	1079	81 43.2	54590
39	2017	8 17.6	7844	54064	7762	1131	81 44.7	54630
40	2018	8 40.6	7830	54098	7740	1181	81 45.9	54662
41	2019	9 04.5	7814	54141	7717	1233	81 47.2	54702
42	2020	9 28.2	7797	54189	7691	1283	81 48.7	54747
43	2021	9 49.5	7780	54238	7666	1327	81 50.2	54793
44	2022	10 12.3	7770	54291	7647	1376	81 51.3	54844

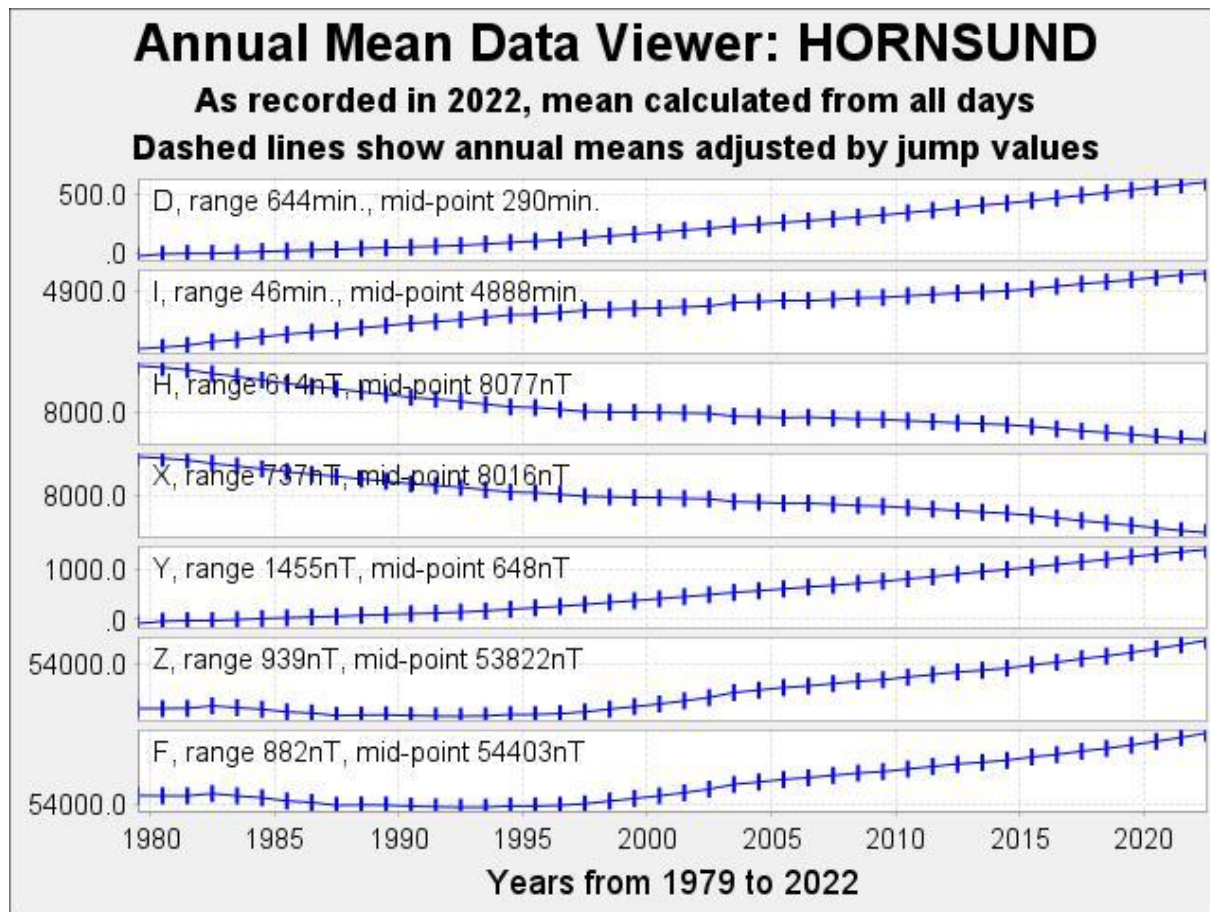
Fig. 13. Secular changes of H , X , Y , Z , F , D and I at Hornsund.

Table 23
Monthly and yearly mean values of magnetic components
HRN 2022

	Jan	Feb	Mar	Apr	May	Jun	Jul	Aug	Sep	Oct	Nov	Dec	Mean
North component: 7500 + ... in nT													
All days	135	134	153	157	175	172	166	159	148	128	122	113	147
Quiet days	152	144	159	163	171	168	178	157	146	139	136	132	154
Disturbed days	109	105	139	143	170	175	126	182	147	110	91	76	131
East component: 1000 + ... in nT													
All days	355	359	362	369	369	374	373	379	386	392	398	402	376
Quiet days	349	355	360	366	366	377	369	383	384	388	393	397	374
Disturbed days	370	367	365	371	377	370	379	366	389	395	407	418	381
Vertical component: 5400 + ... in nT													
All days	277	282	280	287	282	280	274	286	299	312	313	317	291
Quiet days	263	274	277	283	275	268	274	284	297	303	303	309	284
Disturbed days	298	307	270	311	276	283	259	276	320	331	339	341	301

Table 24
 Three-hour-range K indices
 Hornsund, January–March 2022
 The limit of $K = 9$ is 2500

Day	January		February		March	
	K	SK	K	SK	K	SK
1	*855 4787	*	5554 4235	33	5576 5595	47
2	6555 4599	48	8544 4733	38	4455 5334	33
3	5776 4448	45	6957 6577	52	4454 4456	36
4	6654 3334	34	5875 6899	57	6666 5555	44
5	3653 4433	31	5566 6473	42	8567 7668	53
6	3333 2234	23	6776 6597	53	9576 5576	50
7	2232 2112	15	5465 4567	42	7665 6667	49
8	1335 3489	36	5544 5555	38	5653 4455	37
9	7565 4458	44	3543 3237	30	7555 4437	40
10	5643 3886	43	6477 6755	47	6564 5565	42
11	5444 4632	32	7667 3496	48	5577 6658	49
12	2353 4476	34	6565 6677	48	9774 3433	40
13	4434 3453	30	7776 7956	54	3447 9777	48
14	2344 5657	36	7566 6583	46	8455 4446	40
15	7666 6599	54	3445 5442	31	5555 5777	46
16	7776 6499	55	3555 6667	43	3445 4874	39
17	7556 5677	48	6455 6*46	*	4665 5*44	*
18	9565 7698	55	4355 5554	36	64*3 4344	*
19	9976 7*75	*	4645 6648	43	4465 2354	33
20	5554 3324	31	7665 5466	45	4764 4325	35
21	4334 6669	41	3456 7576	43	4343 4424	28
22	7664 5559	47	5666 6346	42	4564 5485	41
23	8775 5423	41	3467 6568	45	3565 5533	35
24	3454 4335	31	8675 4***	*	6556 4523	36
25	5656 5558	45	*466 5336	*	5655 5562	39
26	3566 5679	47	2354 3232	24	4545 4564	37
27	4356 5488	43	3465 4775	41	4557 7777	49
28	4565 4359	41	4565 5454	38	6755 5433	38
29	6766 6325	41			4445 6665	40
30	4665 6448	43			3345 3458	35
31	7655 5554	42			7788 7745	53

Table 25
 Three-hour-range K indices
 Hornsund, April–June 2022
 The limit of $K = 9$ is 2500

Day	April		May		June	
	K	SK	K	SK	K	SK
1	4676 8667	50	6577 6665	48	6666 5445	42
2	8976 6696	57	6554 5564	40	5555 5***	*
3	8664 6865	49	4665 6656	44	*545 5435	*
4	7767 6663	48	5665 6365	42	3454 5355	34
5	4766 6554	43	3674 4444	36	4545 5455	37
6	7555 5564	42	4556 6654	41	5668 7567	50
7	4776 6655	46	3445 5344	32	4876 55*5	*
8	7654 5435	39	6555 5453	38	6466 4475	42
9	6687 6663	48	5675 5443	39	5446 6565	41
10	5998 6577	56	4442 5644	33	5556 64*4	*
11	6767 5653	45	4654 5565	40	5675 5545	42
12	4446 8877	48	6773 765*	*	6768 9777	57
13	6676 5333	39	*566 6555	*	7888 8766	58
14	4677 7877	53	5675 6765	47	6677 7767	53
15	9978 7766	59	6766 6544	44	6899 8956	60
16	4556 7655	43	6787 7674	52	6778 7658	54
17	6777 6755	50	4689 8596	55	8777 7676	55
18	4677 5685	48	7656 6655	46	6687 6779	56
19	5566 6555	43	7786 7676	54	9967 6664	53
20	7666 4336	41	5877 5868	54	5778 9765	54
21	6775 8554	47	8775 7753	49	6687 6576	51
22	5666 5764	45	9788 8644	54	6698 8646	53
23	5668 7667	51	6576 4433	38	6766 6575	48
24	4576 4443	37	3646 6545	39	6543 4457	38
25	3456 6565	40	6777 4564	46	6777 7667	53
26	3354 6433	31	4555 5564	39	8789 8787	62
27	4664 8767	48	3456 7756	43	7885 6376	50
28	7787 7777	57	6798 6444	48	5776 6469	50
29	6978 7666	55	7686 6688	55	6666 6333	39
30	8677 6647	51	8766 6668	53	4465 5345	36
31			7766 7697	55		

Table 26
 Three-hour-range K indices
 Hornsund, July–September 2022
 The limit of $K = 9$ is 2500

Day	July		August		September	
	K	SK	K	SK	K	SK
1	5444 4458	38	776* 5445	*	5786 5444	43
2	8775 6645	48	5767 5667	49	4656 5346	39
3	5444 4565	37	5766 6585	48	7687 8886	58
4	7997 6866	58	5555 6756	44	8779 7988	63
5	5544 4454	35	7544 5437	39	6778 7989	61
6	4465 5554	38	5444 5323	30	8867 8978	61
7	3457 9755	45	4679 7696	54	5677 7964	51
8	7778 6565	51	7778 7778	58	4877 6768	53
9	5534 7655	40	5798 8876	58	6578 5544	44
10	4577 7665	47	5768 7797	56	5777 7775	52
11	4466 7875	47	8877 7876	58	5756 6964	48
12	5799 8776	58	6588 7544	47	6576 5454	42
13	6557 7554	44	4777 7666	50	2545 5423	30
14	4645 6786	46	6766 6442	41	3465 *445	*
15	6648 8867	53	4666 7643	42	6344 4534	33
16	6678 6566	50	4555 6435	37	3545 4533	32
17	5466 5455	40	5757 6897	54	3345 5345	32
18	4677 7587	51	6697 9999	64	5666 6565	45
19	5897 8967	59	6767 6996	56	5556 6665	44
20	5667 6654	45	6774 4357	43	6675 6496	49
21	5567 7877	52	7766 6876	53	5566 6*22	*
22	7676 5555	46	6777 6564	48	24** ****	*
23	7977 5446	49	4445 5335	33	5577 7765	49
24	6776 6675	50	4445 4323	29	5778 7976	56
25	5656 5547	43	4456 6324	34	4566 ****	*
26	8757 5547	48	3554 4454	34	554* ****	*
27	6786 6556	49	5557 7566	46	**** **46	*
28	5784 6686	50	5667 5553	42	443* **44	*
29	5445 6444	36	4776 7554	45	**66 5675	*
30	4566 7545	42	4976 55**	*	6687 7665	51
31	5667 6655	46	*767 6659	*		

Table 27
 Three-hour-range K indices
 Hornsund, October–December 2022
 The limit of $K = 9$ is 2500

Day	October		November		December	
	K	SK	K	SK	K	SK
1	3333 3466	31	3565 5265	37	5876 7999	60
2	4556 5958	47	6655 6665	45	6867 7899	60
3	6675 7787	53	4567 7856	48	5875 5887	53
4	4696 4587	49	5666 5847	47	6555 7799	53
5	6675 6698	53	5755 5456	42	4665 5433	36
6	5677 6699	55	4453 3334	29	3564 6453	36
7	6776 6554	46	3557 5665	42	3456 6657	42
8	3666 7787	50	5554 5744	39	4465 4349	39
9	7877 6996	59	4555 3222	28	9566 4347	44
10	5566 5676	46	3222 2221	16	7755 3485	44
11	4445 5247	35	2354 5445	32	6454 5646	40
12	3455 5476	39	4554 3322	28	4544 4467	38
13	3444 4334	29	3575 6664	42	7343 4333	30
14	4467 6534	39	3445 4463	33	2453 4565	34
15	6666 5586	48	3444 3335	29	3444 3433	28
16	6678 7646	50	2333 3575	31	7444 3363	34
17	4443 5613	30	2323 3133	20	3443 3122	22
18	2355 4458	36	4342 4357	32	2343 4545	30
19	6655 5336	39	6335 3223	27	5755 6544	41
20	4455 7446	39	3344 4554	32	4354 2345	30
21	3656 4234	33	5676 5434	40	4465 4557	40
22	4676 4565	43	4444 3332	27	4454 6697	45
23	5456 5655	41	2352 3333	24	7656 7679	53
24	5566 5334	37	3454 4435	32	6776 6979	57
25	2445 5532	30	3566 6689	49	6655 5788	50
26	2343 4455	30	7666 5696	51	7567 7744	47
27	5655 6563	41	4775 5595	47	8765 5646	47
28	4775 6987	53	7986 5498	56	4655 5336	37
29	7567 8789	57	9866 7777	57	2356 6668	42
30	5656 6655	44	8867 7587	56	9666 8999	62
31	4765 4954	44			6566 *589	*

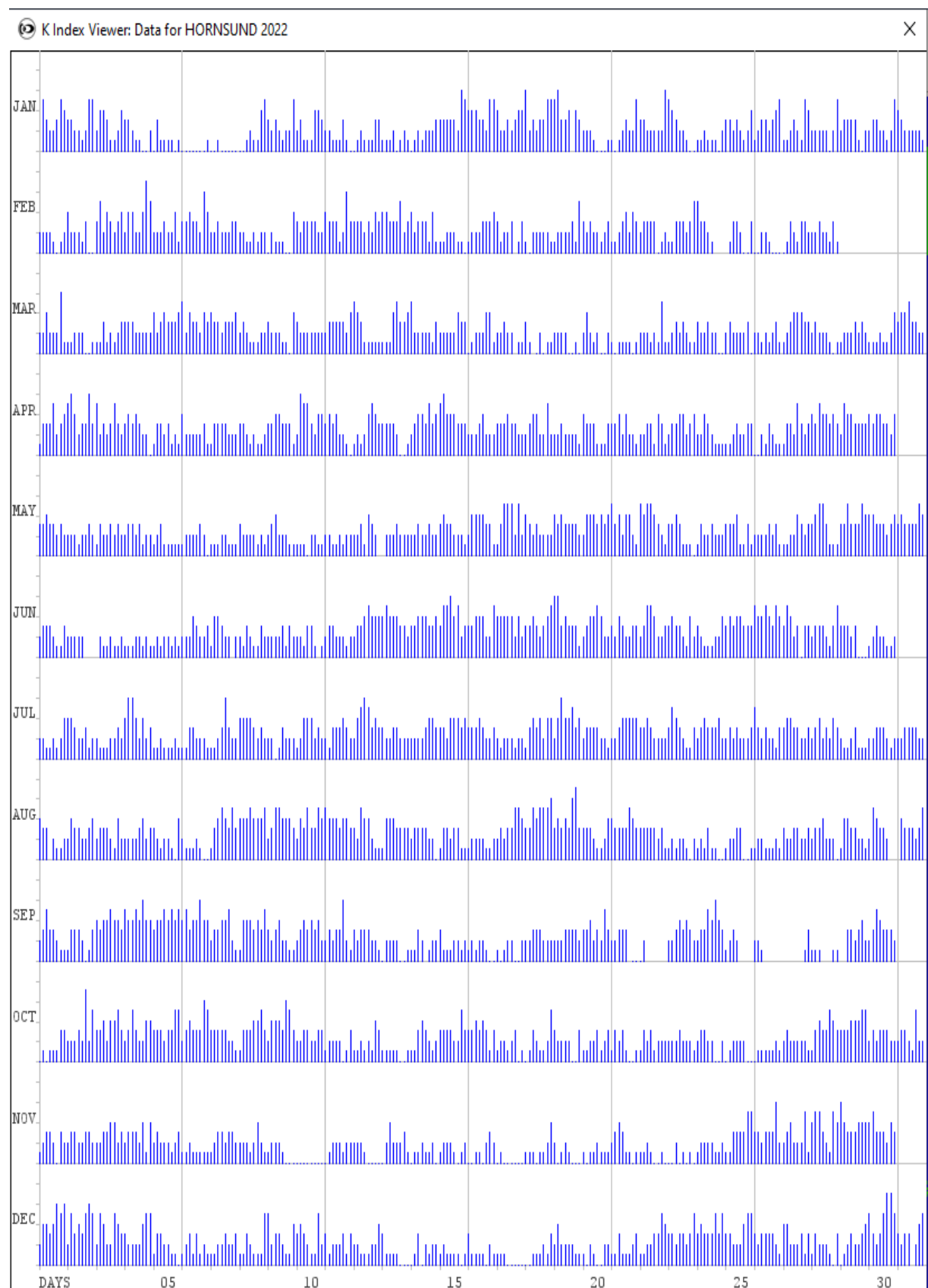


Fig. 14. *K*-indices in graphical form, Hornsund 2022.

A c k n o w l e d g m e n t s

This work is supported by the Ministry of Science and Higher Education of Poland for the statutory activities of the Institute of Geophysics, Polish Academy of Sciences, grant No. 3841/E-41/S/2020 as well as by SPUB funds (Specjalne Urządzenie Badawcze). The study was financially supported by the project called EPOS-PL (No. POIR.04.02.00-14-A003/16) co-financed by the European Union from the funds of the European Regional Development Fund (ERDF).

R e f e r e n c e s

- Geese, A. (2011). Earth's magnetic field: observation and modelling from global to regional scales, Ph.D. Thesis, Tech. Rep. STR, 11/03, Deutsches GeoForschungsZentrum GFZ, Potsdam, DOI: doi.org/10.2312/GFZ.b103-11036.
- Jankowski, J., and C. Sucksdorff (1996), *Guide for Magnetic Measurements and Observatory Practice*, IAGA, Warsaw, 235 pp.
- Jankowski, J., and J. Marianuk (2007), Past and present of Polish geomagnetic observatories, *Publs. Inst. Geophys. Pol. Acad. Sc. C-99 (398)*, 20–31.
- Macmillan, S. (2007), Observatories: an overview. In: *Encyclopedia of Geomagnetism and Paleomagnetism*, 708–711, Springer.
- Neska, M., and G. Satori (2006), Schumann resonance observation at Polish Polar Station at Spitsbergen and Geophysical Observatory in Belsk, *Prz. Geofiz.* **3–4**, 189–198 (in Polish).
- Nowożyński, K., and J. Reda (2007), Comparison of observatory data in quasi-real time, *Publs. Inst. Geophys. Pol. Acad. Sc. C-99 (398)*, 123–127.
- Nowożyński, K., T. Ernst, and J. Jankowski (1991), Adaptive smoothing method for computer derivation of K-indices, *Geophys. J. Int.* **104**, 1, 85–93, DOI: 10.1111/j.1365-246X.1991.tb02495.x.
- Reda, J., and J. Jankowski (2004), Three-hour activity index based on power spectra estimation, *Geophys. J. Int.* **157**, 1, 141–146, DOI: 10.1111/j.1365-246X.2004.02241.x.
- Reda, J., and M. Neska (2007), Measurement Session during the XII IAGA Workshop at Belsk, *Publs. Inst. Geophys. Pol. Acad. Sc. C-99 (398)*, 7–19.

Received 21 November 2023

Accepted 28 November 2023

C O N T E N T S

1. Introduction	1
2. What is observed	1
3. Description of observatories	2
3.1 Central Geophysical Observatory at Belsk, Central Poland	4
3.2 Geophysical Observatory at Hel, Northern Poland	5
3.3 Polish Polar Station Hornsund, Spitsbergen	5
4. Instrumentation	6
4.1 Absolute measurements	6
4.2 Recording of geomagnetic field variations	8
4.3 Calibration of magnetic sensors	10
4.4 Data processing	11
4.5 Data availability	12
5. Contact persons, postal addresses, contact details	13
5.1 Belsk Observatory	13
5.2 Hel Observatory	13
5.3 Hornsund Observatory	13
6. Personnel taking part in the work of Belsk, Hel, and Hornsund Observatories in 2022 ...	13
7. Tables and plots for Belsk Observatory	14
8. Tables and plots for Hel Observatory	26
9. Tables and plots for Hornsund Observatory	35
Acknowledgments	43
References	43

"Publications of the Institute of Geophysics, Polish Academy of Sciences: Geophysical Data Bases, Processing and Instrumentation" appears in the following series:

A – Physics of the Earth's Interior

B – Seismology

C – Geomagnetism

D – Physics of the Atmosphere

E – Hydrology (formerly Water Resources)

P – Polar Research

M – Miscellanea

Every volume has two numbers: the first one is the consecutive number of the journal and the second one (in brackets) is the current number in the series.

